การดัดแปรเส้นใยสับปะรดและการประยุกต์ในการนำส่งยา

นายอดิศร ตรีมรรค

วิทยานิพนธ์นี้เป็นส่วนหนึ่งของการศึกษาตามหลักสูตรปริญญาวิทยาศาสตรมหาบัณฑิต
สาขาวิชาปิโตรเคมีและวิทยาศาสตร์พอลิเมอร์
คณะวิทยาศาสตร์ จุฬาลงกรณ์มหาวิทยาลัย
ปีการศึกษา 2557

MODIFICATION OF PINEAPPLE FIBER AND APPLICATION IN DRUG DELIVERY

Mr. Adison Treemak

A Thesis Submitted in Partial Fulfillment of the Requirements

for the Degree of Master of Science Program in Petrochemistry and Polymer Science

Faculty of Science

Chulalongkorn University

Academic Year 2014

Thesis Title	MODIFICATION OF PINEAPPLE FIBER AND APPLICATION IN DRUG DELIVERY
By	Mr. Adison Treemak
Field of Study	Petrochemistry and Polymer Science
Thesis Advisor	Associate Professor Supason Wanichwecharungruang, Ph.D.

Accepted by the Faculty of Science, Chulalongkorn University in Partial Fulfillment of the Requirements for the Master's Degree

.....Dean of the Faculty of Science
(Professor Supot Hannongbua, Dr.rer.nat.)

THESIS COMMITTEE

.....Chairman
(Assistant Professor Warinthorn Chavasiri, Ph.D.)

.....Thesis Advisor
(Associate Professor Supason Wanichwecharungruang, Ph.D.)

.....Examiner
(Assistant Professor Amarawan Intasiri, Ph.D.)

.....External Examiner
(Assistant Professor Thitinan Karpkird, Ph.D.)

อดิศร ตรีมรรค : การดัดแปรเส้นใยสับปะรดและการประยุกต์ในการนำส่งยา (MODIFICATION OF PINEAPPLE FIBER AND APPLICATION IN DRUG DELIVERY) อ. ที่ปรึกษาวิทยานิพนธ์หลัก: รศ. ดร.ศุภศร วนิชเวชารุ่งเรือง, 72 หน้า.

ในปัจจุบันของเสียทางการเกษตรได้กลายเป็นปัญหาด้านสิ่งแวดล้อมในหลายประเทศ ตามที่องค์การอาหารและการเกษตรแห่งสหประชาชาติได้รายงานว่ากากสับปะรดในประเทศไทยมีมากกว่า 189 กิโลตัน งานวิจัยนี้ศึกษาการดัดแปรทางเคมีของเส้นใยเซลลูโลสในกากสับปะรดจากกระบวนการผลิตน้ำสับปะรดและการประยุกต์ใช้เป็นวัสดุในการนำส่งยา โดยเส้นใยสับปะรดจะถูกทำปฏิกิริยาออกซิเดชันด้วยโซเดียมเมตาเพอริโอเดตได้เป็นไดอัลดีไฮด์เซลลูโลสที่สามารถละลายน้ำได้ ซึ่งพบว่าภาวะที่เหมาะสมในการออกซิไดส์เซลลูโลสคือโซเดียมเมตาเพอริโอเดต 0.137 โมลาร์ เป็นเวลา 15 ชั่วโมง ที่อุณหภูมิ 55 องศาเซลเซียส พอลิเมอร์ที่ได้สามารถละลายน้ำได้ดี นอกจากนี้เซลลูโลสที่ได้สามารถสร้างพันธะชิฟเบสระหว่างหมู่อัลดีไฮด์บนสายโซ่ของพอลิเมอร์กับหมู่อะมิโนบนยาไมน็อกซิดิล อนุภาคนาโนของเซลลูโลสที่กักเก็บยาไมน็อกซิดิลมีความเสถียรและมีขนาดเส้นผ่านศูนย์กลางในช่วง 110 ถึง 300 นาโนเมตร มีประสิทธิภาพการกักเก็บยาไมน็อกซิดิลมากกว่า 88% และมีความสามารถในการบรรจุประมาณ 85% ระบบนี้แสดงให้เห็นถึงการปลดปล่อยยาไมน็อกซิดิลออกจากอนุภาคอย่างช้า ๆ ในสารละลายบัฟเฟอร์โซเดียมอะซิเตต (พีเอช 5.5 และอุณหภูมิ 37 องศาเซลเซียส) จากงานวิจัยนี้ คาดว่าอนุภาคที่เตรียมได้จะสามารถนำไปใช้ในการรักษาผมร่วงได้ในอนาคต

สาขาวิชา ปิโตรเคมีและวิทยาศาสตร์พอลิเมอร์ ลายมือชื่อนิสิต .....

ปีการศึกษา 2557 ลายมือชื่อ อ.ที่ปรึกษาหลัก .....

5572166223 : MAJOR PETROCHEMISTRY AND POLYMER SCIENCE
KEYWORDS: PINEAPPLE / WASTE / CELLULOSE / SODIUM METAPERIODATE / MINOXIDIL

ADISON TREEMAK: MODIFICATION OF PINEAPPLE FIBER AND APPLICATION IN DRUG DELIVERY. ADVISOR: ASSOC. PROF. SUPASON WANICHWECHARUNGRUANG, Ph.D., 72 pp.

At present, the agro-waste has become an environmental issue in many countries. According to Food and Agricultural Organization (FAO), reported that a pineapple waste in Thailand is more than 189 kilotons. This research investigated the chemical modification of cellulose fiber in the pineapple waste from pineapple juice production, in order to use as drug carrier material. Pineapple fiber waste was oxidized by sodium metaperiodate to obtain dialdehyde soluble cellulose. The optimized condition for the oxidation was 15 h treatment of the fiber with 0.137 M sodium metaperiodate at 55°C. The obtained polymer could dissolve well in aqueous medium and form Schiff base with amino group on minoxidil. The minoxidil-grafted dialdehyde soluble cellulose nanoparticles self-assembled into stable nanoparticles with hydrodynamic diameters in the range of 110 to 300 nm. The encapsulation efficiency of minoxidil by the obtained cellulose was more than 88%, with the loading capacity of 85%. The prolonged drug release of minoxidil could be achieved when tested in acetate buffer solution pH 5.5, 37°C. It is expected that the obtained particles could be further developed for an androgenic alopecia treatment in the future.

Field of Study: Petrochemistry and Polymer Science Student's Signature .....
Advisor's Signature .....

Academic Year: 2014

ACKNOWLEDGEMENTS

First of all, I would like to express my sincere appreciation to my thesis advisor, Associate Professor Dr. Supason Wanichwecharungruang for her helpful supervision, invaluable assistance and generous encouragement to fulfill my achievement.

I would like to thank all members of the committee Assistant Professor Dr. Warinthorn Chavasiri, Assistant Professor Dr. Amarawan Intasiri and Assistant Professor Dr. Thitinan Karpkird for their time and suggestions as the committee members.

I also sincerely thank Tipco Company, Beta Pharma Company and Welltech Biotechnology (Lab) Company for materials support and I would like to thank the Graduate School, Chulalongkorn University for financial support.

Finally, I would like to specially thank the most important persons in my life, my family, my friends and research group members for their support, encouragement and advice throughout my Master study.

CONTENTS

Page

THAI ABSTRACT iv

ENGLISH ABSTRACT v

ACKNOWLEDGEMENTS vi

CONTENTS vii

LIST OF TABLES ix

LIST OF FIGURES x

LIST OF ABBREVIATIONS xiii

CHAPTER I INTRODUTION 1

1.1 Pineapple 1

1.1.1 History and morphology of pineapple 1

1.2 Carriers in drug delivery system 4

1.2.1 Cellulose 5

1.3 Chemical modification of cellulose 6

1.3.1 Periodate oxidation of cellulose 7

1.4 Literature reviews of oxidation of cellulose and biodegradation 9

1.5 Minoxidil 12

1.6 Literature reviews of carrier in encapsulated-minoxidil system 13

1.7 Research goal 18

CHAPTER II EXPERIMENTAL 19

2.1 Materials and Chemicals 19

2.2 Preparation of dialdehyde soluble cellulose 19

2.3 Preparation of minoxidil-grafted dialdehyde soluble cellulose 22

Page

2.4 Characterization of minoxidil-grafted dialdehyde soluble cellulose 23
2.5 The release of minoxidil from Schiff base nanoparticles 25
2.6 The release of minoxidil from Schiff base nanoparticles 26
CHAPTER III RESULTS AND DISCUSSION 27
3.1 Preparation and characterization of dialdehyde soluble cellulose 27
3.2 Preparation of minoxidil-grafted dialdehyde soluble cellulose 32
3.3 Characterization of minoxidil-grafted dialdehyde soluble cellulose 35
3.4 Controlled release study of minoxidil 40
CHAPTER IV CONCLUSION 42
REFERENCES 43
APPENDIX A 50
APPENDIX B 52
APPENDIX C 56
APPENDIX D 59
APPENDIX E 61
APPENDIX F 63
APPENDIX G 66
VITA 72

LIST OF TABLES

Table 1.1 The chemical compositions of the pineapple residues (g/100g dry weight) [12]..... 3

Table 2.1 Minoxidil-grafted dialdehyde soluble cellulose ratios. 23

Table 3.1 Maximum amounts of minoxidil loading in various 33

Table B1 sodium metaperiodate concentration and its corresponding absorbance value at 222 nm..... 52

Table F1 minoxidil concentration and its corresponding absorbance value at 289 nm 63

Table G1 minoxidil concentration and its corresponding absorbance value at 287 nm..... 66

LIST OF FIGURES

Figure 1.1 Pineapple fruits “Smooth Cayenne” [2] 1

Figure 1.2 Pineapple canned production [3] 2

Figure 1.3 Two types of polymeric nanoparticles (nanosphere and nanocapsule) [15] 4

Figure 1.4 Chemical structure of cellulose [23] 5

Figure 1.5 Chemical modification of cellulose [28] 7

Figure 1.6 Synthesis of 2,3-dialdehyde cellulose [33] 8

Figure 1.7 The oxidation mechanism of cellulose [34] 8

Figure 1.8 Degradation of partially oxidized alginate in pH 7.4 at 37°C [35] 9

Figure 1.9 Structure of crosslinking collagen with dialdehyde cellulose [36] 10

Figure 1.10 The chemistry of periodate oxidation and alkaline degradation of alginate [37] 11

Figure 1.11 Preparation nanofibrillation of hardwood cellulose [38] 12

Figure 1.12 Chemical structure of minoxidil [41] 13

Figure 1.13 The skin permeation of minoxidil through porcine skin from different liposomal formulation: -■- EU-coated liposomes; -◊- CS-coated liposomes; -○- DPPC liposomes [45] 15

Figure 1.14 Albino rat skin treated with adopted formulation at day 20 (A) and at day 30 after the treatments (B). Commercial 5% minoxidil solution at day 20 (C) and at day 30 after the treatments (D). Blank formulation at day 20 (E) and at day 30 after the application (F). No drug as control group at day 20 (G) and at day 30 after application to the skin (H). [47] 16

Figure 1.15 Schiff base formation [48] 17

Figure 2.1 Synthesis of dialdehyde soluble cellulose 19

Figure 2.2 Synthesis of dialdehyde soluble cellulose 22

Figure 3.1 Synthesis of dialdehyde soluble cellulose 27

Figure 3.2 (a) The picture of dialdehyde soluble cellulose product in solution and (b) dry form 28

Figure 3.3 Percent yield (blue line), Percent of aldehyde content (green line) and molecular weight (black line) of dialdehyde soluble cellulose and Percent of leftover sodium metaperiodate (red line) in the reaction. 29

Figure 3.4 The ATR-FTIR spectrums of bleached pineapple fiber (pink line) and dialdehyde soluble cellulose at various times 3 h (black line), 6 h (blue line), 15 h (red line) and 24 h (green line) 30

Figure 3.5 X-ray powder diffraction patterns of pineapple fiber (black line) and dialdehyde soluble cellulose (red line) 31

Figure 3.6 The mechanism of Schiff base formation [51] 32

Figure 3.7 Schematic representation of minoxidil-grafted dialdehyde soluble cellulose nanoparticle 34

Figure 3.8 (a) minoxidil-grafted dialdehyde soluble cellulose solution and (b) dry product obtained at 1: 7 (wt/wt) of polymer: minoxidil ratio 34

Figure 3.9 ATR-FTIR spectra of dialdehyde soluble cellulose (red line), minoxidil (blue line) and minoxidil-grafted dialdehyde soluble cellulose (green line) 35

Figure 3.10 SEM photographs of minoxidil-grafted dialdehyde soluble cellulose nanoparticles at polymer concentration of 10 ppm (a) at 25,000x magnification and (b) at 50,000x magnification 36

Figure 3.11 SEM photographs of (a) the excess precipitate of minoxidil in samples 8: 1 (w/w) of drug to polymer ratio and (b) unencapsulated minoxidil 36

Figure 3.12 TEM photograph of minoxidil-grafted dialdehyde soluble cellulose nanoparticles at polymer concentration of 10 ppm 37

Figure 3.13 Size distributions of (a) unloaded particles and (b) minoxidil-grafted cellulose nanoparticles 38

Figure 3.14 Zeta potential of (a) unloaded particles and (b) minoxidil-grafted cellulose nanoparticles 38

Figure 3.15 Thermo gravimetric analysis (TGA) curves of dialdehyde soluble cellulose (black line), minoxidil (blue line) and minoxidil-grafted cellulose nanoparticles (red line) 39

Figure 3.16 Derivative thermo gravimetric analysis (DTG) curves of dialdehyde soluble cellulose (black line), minoxidil (blue line) and minoxidil-grafted cellulose nanoparticles (red line) 40

Figure 3.17 Release profile of minoxidil from the nanoparticles in acetate buffer solution (pH 5.5) at the indicated times (0, 0.5, 1, 2, 3, 4, 5, 6 and 24 hours) 41

Figure B1 Calibration curve of sodium metaperiodate at 222 nm 52

Figure D1 GPC chromatogram of dialdehyde soluble cellulose at 3 h 59

Figure D2 GPC chromatogram of dialdehyde soluble cellulose at 6 h 59

Figure D3 GPC chromatogram of dialdehyde soluble cellulose at 15 h 59

Figure D4 GPC chromatogram of dialdehyde soluble cellulose at 24 h 60

Figure E1 Thermo gravimetric analysis (TGA) curves of dialdehyde soluble cellulose 61

Figure E2 Thermo gravimetric analysis (TGA) curves of minoxidil 61

Figure E3 Thermo gravimetric analysis (TGA) curves of minoxidil-grafted cellulose nanoparticles 62

Figure F1 Calibration curve for release study of minoxidil in in deionized water at 289 nm 63

Figure G1 Calibration curve for release study of minoxidil in ABS pH 5.5 at 287 nm .. 66

LIST OF ABBREVIATIONS

%	percent
°C	degree Celsius
h	hour
g	gram
min	minute
w/v	weight by volume
w/w	weight by weight
v/v	volume by volume
ppm	parts per million
rpm	revolution per minute
mg	milligram
L	liter
mL	milliliter
µL	microliter
M	molar
mV	millivolt
M_W	molecular weight
Da	Dalton
KHz	kilohertz
cm^{-1}	unit of wavenumber (IR)
cm	centimeter
nm	nanometer

CHAPTER I

INTRODUTION

1.1 Pineapple

The Pineapple (*Ananas comosus L. Merr*) in the Bromeliaceae family embraces about 2,000 species. There are 5 main groups of pineapple popularly grown in the world. Two of these, Queen and Smooth Cayenne, are widely cultivated in South Africa. Queen pineapple has a golden yellow appearance, less juicy and is cultivated for fresh serve only. The Smooth Cayenne is used for canning and juice production because it has high sugar content and suitable canning quality (Figure 1.1) [1].

Figure 1.1 Pineapple fruits “Smooth Cayenne” [2]

1.1.1 History and morphology of pineapple

The plant is innate in South America and said to originate from the area between southern Brazil and Paraguay. In 1495, Christopher Columbus came to the Caribbean and discovered the pineapple. He called it “Pine of The Indies” and brought it back to Europe, later they added the word “apple” because they thought

that it was associated with another tasty fruit and the name of pineapple have been changed ever since [3, 4].

The end of the 19th century, thread industries of pineapple were started in Hawaii. Hawaii Pineapple Company (Dole) was established in 1901 and in 1911 Henry Ginaca invented a machine that produced canned pineapple at the speed up to 100 pineapples per minute. Pineapple products of export are fresh fruit, canned slices, chunk, titbits, crush, spears and juice concentrate (Figure 1.2) [3].

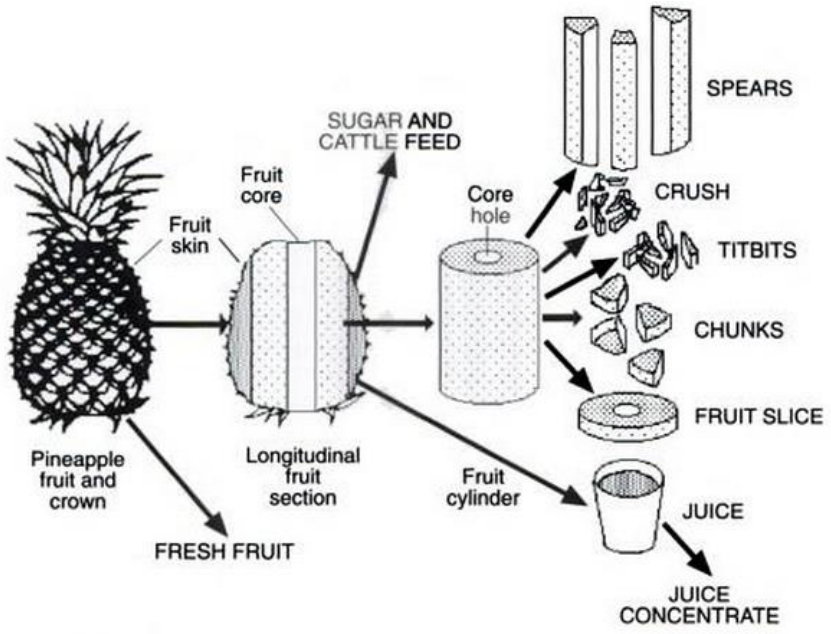

Figure 1.2 Pineapple canned production [3]

Pineapple is one of the most popular tropical fruits in the world and occupies an economically important fruits in Thailand [5]. In 2000-2013, the United Nation reported that the production of pineapple in Thailand was more than 2 million tons per year and Thailand had become the largest producer and exporter of pineapple in Southeast Asia [6]. Pineapple can be used to produce many food products such as canned pineapple, pineapple jam and pineapple juice. Thailand exports 520,000 tons of canned pineapple and 150,000 tons of pineapple juice [7]. In pineapple processes, agro-waste of pineapple residues is left over after cultivation and during canned

pineapple production processes. Due to increasing of pineapple production, the pineapple wastes are also proportionally increasing. Hence, an efficient reuse of these wastes, not only to minimize the environmental impact, but also to obtain a higher profit [8].

Nowadays, the agro-waste has become an environmental issue in many countries since there is no proper method to manage these residues. The pineapple residues are fibrous residue of crowns, leaf, slips, stems and peels in pineapple industry. These wastes are up to 50% (w/w) of total pineapple weight [7, 9]. In 2014, Kiran *et al.* [10] reported that a pineapple waste in Thailand is up to 189.5 kilotons. Large amount of pineapple waste has been sold at very low prices for supplementary as animal feed. However, the pineapple residues were found to have a potential to be converted into valuable products. The pineapple fiber waste contains cellulose as the main component (Table 1.1). Several processes have been utilized pineapple fiber as a raw material to produce paper, textiles, composites and extraction of cellulose fiber [11]. However, there are not many previous reports on the application of cellulose from pineapple fiber waste as a drug carrier.

Table 1.1 The chemical compositions of the pineapple residues (g/100g dry weight) [12].

Fiber	Leaf bracts	Shell	Core
Insoluble dietary fiber	43.53 ± 0.93	46.20 ± 0.50	42.92 ± 0.09
Soluble dietary fiber	29.16 ± 0.46	35.67 ± 0.37	21.27 ± 0.61
Total dietary fiber	74.69	81.8	64.19
Cellulose	43.53 ± 1.17	40.55 ± 1.02	24.53 ± 1.68
Hemicellulose	21.88 ± 0.22	28.69 ± 0.35	28.53 ± 1.37
Lignin	13.88 ± 1.70	10.01 ± 0.38	5.78 ± 0.429
Pectin	2.32 ± 0.37	2.49 ± 0.20	1.58 ± 0.17

1.2 Carriers in drug delivery system

Poor solubility in water and insufficient bioavailability of many drugs are the main problems in drug formulation and drug delivery system. Drug encapsulation is important innovation in a term of materials to develop a drug carrier system to enhance drug solubility, drug delivery systems and control release. Drug-encapsulated into nanoparticles can be defined as a device or a formulation that is capable of introducing a therapeutic substance into the body in a manner that reduces risk of toxicity, patient pain and enhances efficiency [13, 14]. The nanoparticle is divided into two main groups: nanosphere and nanocapsule (Figure 1.3). Nanosphere is a matrix type particle which drugs are loaded within the particle matrix or absorbed at the sphere surface. On the other hand, nanocapsules, a vesicular system, in which the drug is confined to a cavity consisting of an inner liquid core surrounded by a polymeric shell [14].

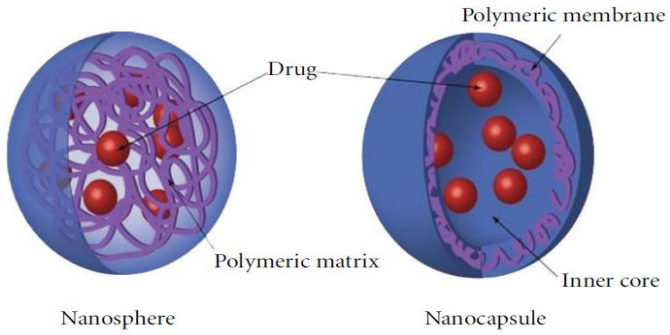

Figure 1.3 Two types of polymeric nanoparticles (nanosphere and nanocapsule) [15]

The polymeric nanoparticles have become interesting in the field of drug delivery because they can encapsulate various substances such as natural active agent, vaccines, hydrophobic molecule etc. The encapsulation process can help protecting and increasing the stability of drug against the harsh environment, increasing the solubility in aqueous phase, enhancing absorption, bioavailability and providing controlled release characteristic. Many encapsulating materials were applied in drug encapsulation system, for instance, vegetable gums, celluloses and

its derivatives, condensation polymers, homopolymers, copolymers, proteins etc. The applied materials should be stable, non-toxic, biocompatible, biodegradable, inert to the loaded drugs and soluble in an aqueous phase [13]. Among these, celluloses are the popular polymer widely employed as an encapsulating material in nanoencapsulation.

1.2.1 Cellulose

Cellulose is a sustainable, abundant renewable biopolymer produced by plants and algae as a constituent of their primary cell walls, and also presents in various natural fibers such as cotton and linen as their main constituent [16-20]. It consists of anhydro-D-glucopyranose units (AGU) linked together through an oxygen covalently bond to C1 of one glucose ring and C4 of the adjoining ring (β-1, 4 linkage) [21]. The chemical structure of cellulose is presented in Figure 1.4. Each monomer unit has three hydroxyl groups per AGU providing an ability to form hydrogen bondings (dotted line in Figure 1.4) [21-23]. The intra and inter-chain interaction between hydroxyl groups can promote an arrangement into high crystallinity structure, resulting in aqueous insolubility and β-1, 4 linkages effect enzymatical undegradablility in the human body or resistant to digestive hydrolysis [21, 24-26].

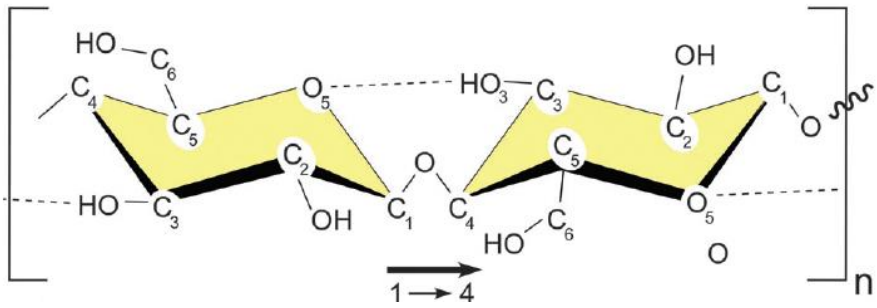

Figure 1.4 Chemical structure of cellulose [23]

The cellulose possesses many advantages to be used as a drug carrier material including [27].

1. Biopolymer
2. Biocompatibility
3. Biodegradability
4. White color, odorlessness and tastelessness
5. Stability against light, heat, oxygen, wetness and chemical
6. Non-toxicity and non-irritant
7. High melting point 500 °C
8. Low cost

1.3 Chemical modification of cellulose

Cellulose has specific and advantageous physical, chemical and biological properties. Chemical modification techniques of cellulose have been investigated to enhance its original properties or to add new functionalities. General ways to perform the chemical modifications or derivatizations of cellulose are esterification and etherification at hydroxyl groups of cellulose. Cellulose derivatives showing water-soluble or organic solvent-soluble properties are prepared by substitution reactions. Others are ion and radical grafting, deoxyhalogenation, acetalation and oxidation. The original properties of cellulose are drastic changed by these chemical modifications. Figure 1.5 shows all common chemical modification approaches of cellulose structure [28].

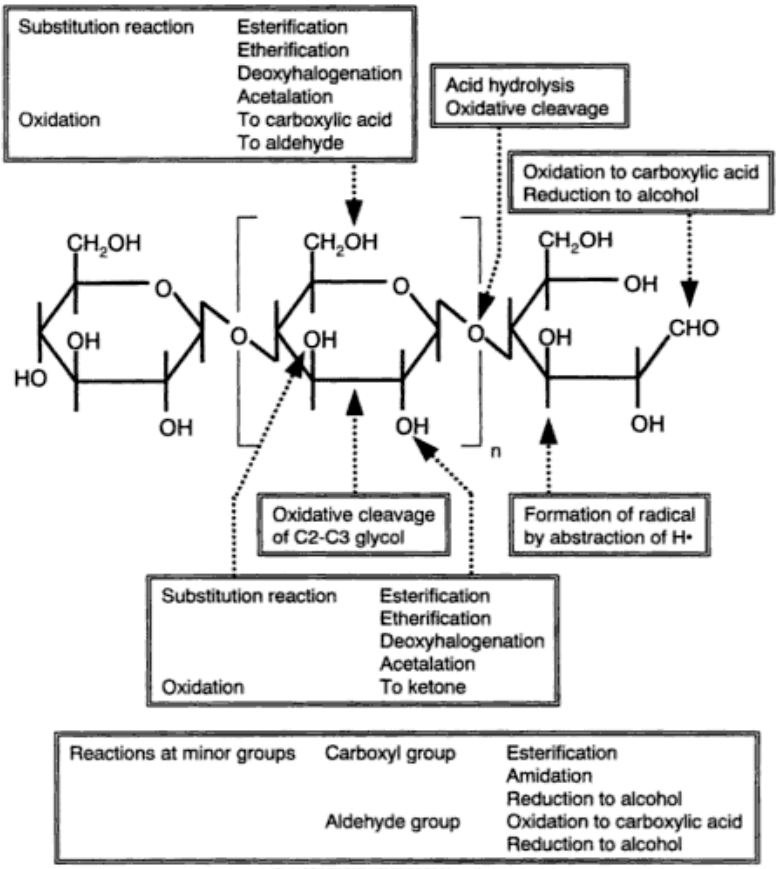

Figure 1.5 Chemical modification of cellulose [28]

1.3.1 Periodate oxidation of cellulose

Cellulose has low reactivity due to the number of hydrogen bonds which restrict its solubility in all common solvents. Cellulose can be made susceptible to hydrolysis by introducing chemical modification [17, 26]. Oxidation of cellulose can be accomplished through the Malaprade reaction. Sodium metaperiodate ($NaIO_4$) is used as a highly specific oxidizing reagent to cleave C-2 and C-3 vicinal dihydroxyl bond of cellulose and oxidize them into 2,3-dialdehyde units, along the cellulose chain without the simultaneous occurrence of side reactions to any great extent (Figure 1.6) [26, 29-31]. The oxidized cellulose readily disperses in water and form thixotropic dispersion. The presence of dialdehyde groups in cellulose after periodate oxidation also improves biodegradability in vivo and in vitro [32], there be giving a large potential to be used in many applications.

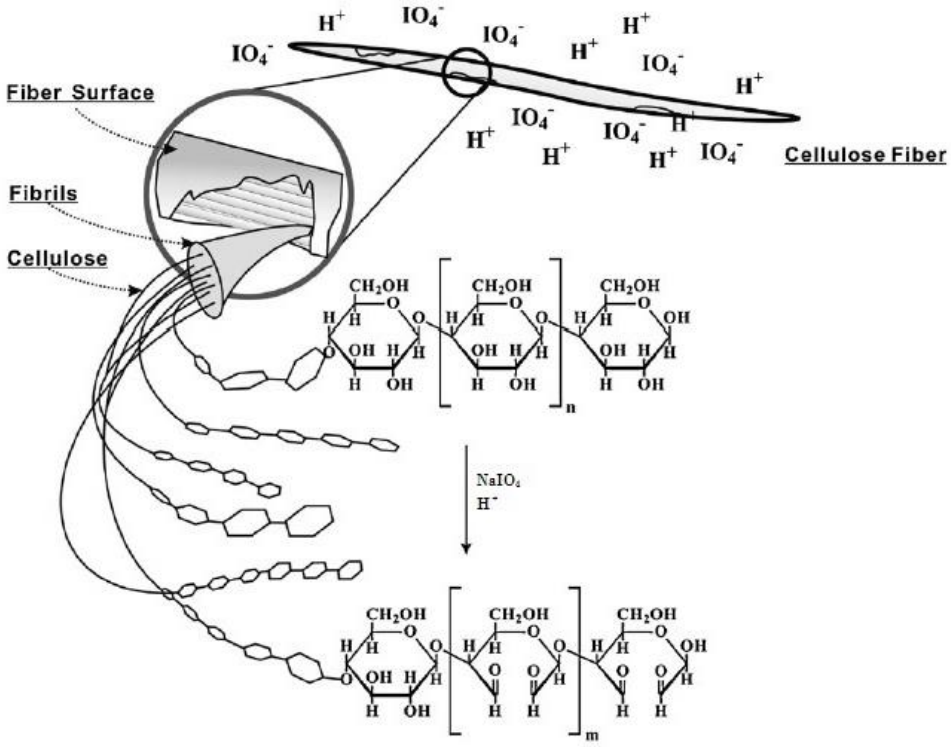

Figure 1.6 Synthesis of 2,3-dialdehyde cellulose [33]

The oxidation mechanism of cellulose starts with an iodine in $NaIO_4$ bonding to both alcohol groups to form a cyclic periodate ester, following by a rearrangement of electron and the cyclic periodate ester is broken down, resulting in the cleavage of the C-C bond to give the dialdehyde (Figure 1.7) [34].

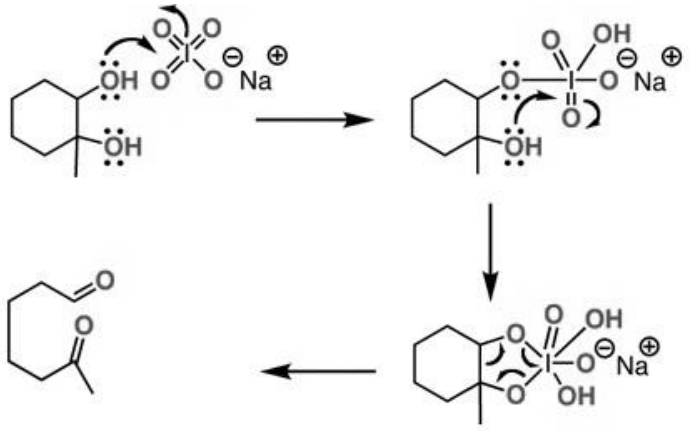

Figure 1.7 The oxidation mechanism of cellulose [34]

1.4 Literature reviews of oxidation of cellulose and biodegradation

In 1982, Singh *et al*. [26] prepared a degradable biopolymer by chemical modification. Oxidation by sodium metaperiodate was highly specific to 1,2-dihydroxyl group and dialdehyde cellulose is generated without the simultaneous occurrence of side reactions. The degree of oxidation reaction depended on the concentration of sodium metaperiodate, ratio of cellulose to sodium metaperiodate solution and reaction time. The oxidized cellulose degraded *in vivo* at pH 7.4 which is approximate to physiological pH.

In 2001, Bouhadir *et al*. [35] studied degradation of oxidized alginate and applied for tissue engineering. The sodium alginate solution was oxidized by sodium metaperiodate at room temperature for 24 h. The obtained 5% oxidized alginate was degraded up to 80% in PBS solution (pH 7.4, 37°C) within 9 days. In vivo studies of alginate-chondrocytes, implantation into the dorsal of mice showed cell distributed throughout the constructs and a new cartilage-like tissue formation.

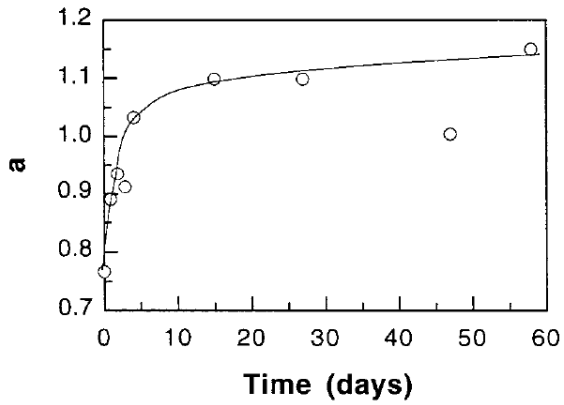

Figure 1.8 Degradation of partially oxidized alginate in pH 7.4 at 37°C [35]

In 2002, Varma *et al.* [29] investigated the effects of the concentration of sodium metaperiodate, reaction time, temperature and pH of the reaction mixture on the percent yield of the oxidation. The increase of the concentration of periodate, reaction time and temperature caused significant enhancement of the %

conversion of cellulose to dialdehyde cellulose. But no significant improvement of percent yield in buffer solution of pH 2-5. Reaction at 55 ℃ gave the highest extent of cellulose oxidation.

In 2007, Hou *et al.* [31] prepared dialdehyde cellulose fibers by sodium metaperiodate oxidation. Kraft softwood pulp sheet fiber was oxidized in three different concentrations of sodium metaperiodate of 0.04, 0.08 and 0.06 mole/L at 45 ℃ for 10, 30, 60, 120, 240, 360 and 480 min, respectively. The obtained fiber was investigated for aldehyde content, degree of crystallinity, polymerization and fiber length. The results showed aldehyde content increased as the sodium metaperiodate concentration and oxidation time increased, but degree of crystallinity, degree of polymerization and fiber length of oxidized fiber deceased when oxidant concentration and oxidation time increased. The oxidation of cellulose fiber showed enhanced water absorbency property and can be applied to use in tissue or wet wipes production.

In 2009, Kanth *et al.* [36] prepared dialdehyde cellulose by sodium metaperiodate oxidation in the dark at 35 ℃ for 48 h. The obtained dialdehyde cellulose was crosslinked with type I collagen from rat tail tendon to enhance stability of the matrix. The results showed that 92% dialdehyde content of oxidized cellulose crosslinked with collagen was resistant to thermal and enzymatic degradation. The collagen matrix showed increased denaturation temperature (from 64 to 82 ℃) and reached 93% resistance to collagenolytic hydrolysis.

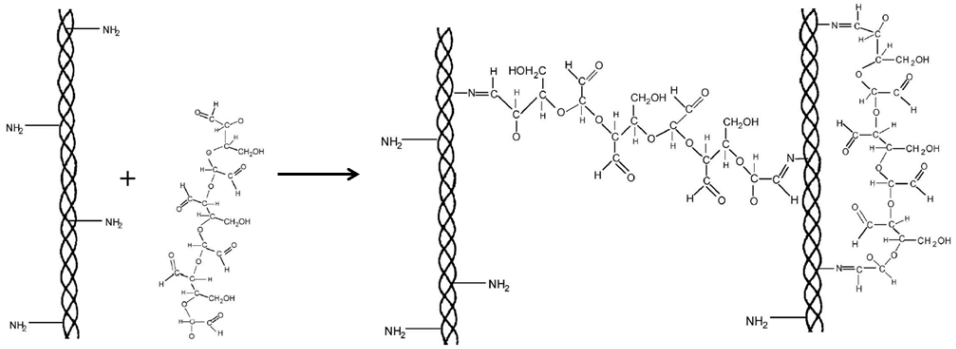

Figure 1.9 Structure of crosslinking collagen with dialdehyde cellulose [36]

In 2011, Kristiansen *et al.* [37] studied periodate oxidation and degradation behavior of alginates. The result showed that degradation of oxidized alginate in pH 7.2 buffer increased when degree of oxidation increased. Eight percents of oxidized alginate were degraded at the rate of 6.4- fold faster than the unoxidized alginate.

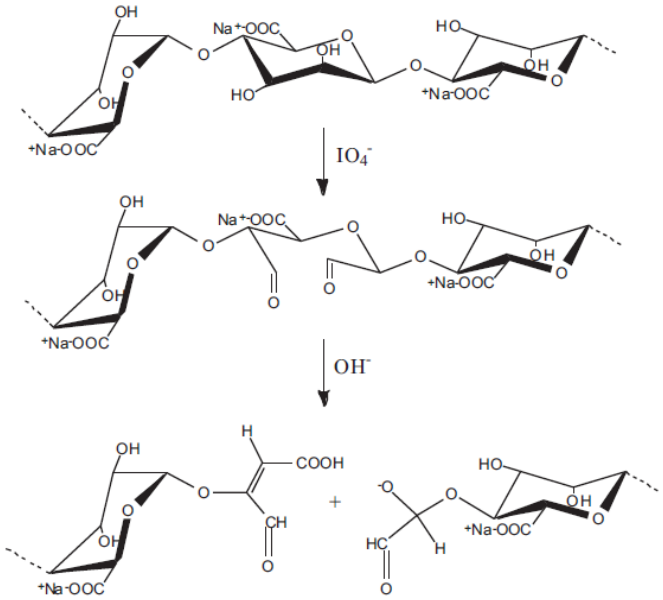

Figure 1.10 The chemistry of periodate oxidation and alkaline degradation of alginate [37]

In 2012, Liimatainen *et al.* [38] prepared nanofibrillation of hardwood cellulose pulp through sequential sodium metaperiodate-chlorite oxidation. The cellulose pulp was treated with sodium metaperiodate at 55 °C for various time, and further reacted with sodium chlorite at room temperature for 48 h. The oxidized cellulose was suspended in deionized water by homogenizer. The result showed carboxyl content increased when oxidization time of cellulose increased. The obtained nanofibril suspension of 2,3-dicarboxylic acid cellulose was transparent.

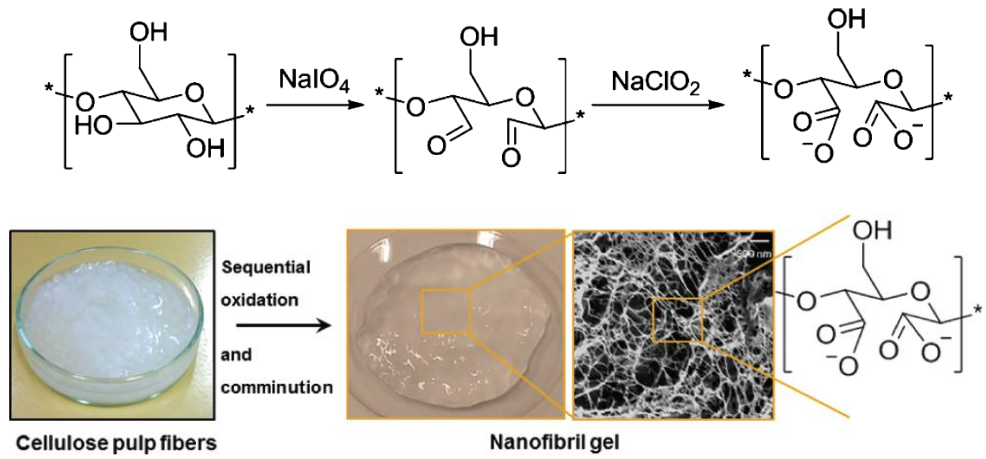

Figure 1.11 Preparation nanofibrillation of hardwood cellulose [38]

The oxidation of cellulose possesses many advantages and has already been demonstrated in various applications. But there is no report on modification of cellulose fiber from pineapple waste and the use of the oxidized cellulose as drug carrier.

1.5 Minoxidil

Minoxidil (6-Piperidin-1-ylpyrimidine-2,4-diamine-3-oxide, Figure 1.12), a piperidino-pyrimidine derivative, is an oral vasodilating drug, which has potent effects on circulating of blood in vascular. Minoxidil demonstrates the antihypertensive activity by decrease in peripheral resistance due to vasodilation [39]. The frequency of hypertrichosis (dramatic increase in hair growth) prompted the consideration of using minoxidil as a hair growth. Mechanistic studies of minoxidil induced hair claimed that the hair follicle produced minoxidil sulfate as an active metabolite that stimulated hair growth [40]. Minoxidil has been widely used for treatment of androgenic alopecia in both men and women. The US Food and Drug Administration approved treatments for androgenic alopecia at a dose of 1 mg per day and topical solutions of 2 and 5% [41]. Minoxidil is poorly soluble in water and most of water-

immiscible organic solvents. Therefore, commercial products of minoxidil usually contain high percentage of ethyl alcohol and/or propylene glycol. These organic solvents can lead to severe adverse effects such as scalp dryness, scaling, redness, irritation and allergic contact dermatitis [42].

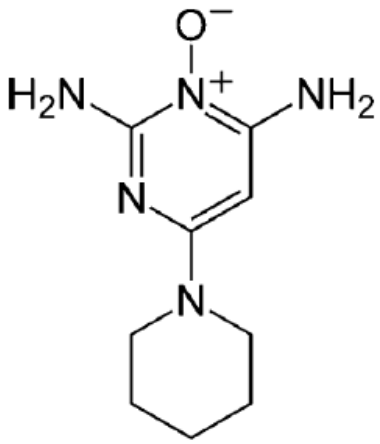

Figure 1.12 Chemical structure of minoxidil [41]

1.6 Literature reviews of carrier in encapsulated-minoxidil system

In 2004, Shim *et al.* [43] synthesized poly(**ε**-caprolactone)-block-poly(ethyleneglycol) to encapsulate minoxidil through solvent evaporation method. The two main average sizes of the nanoparticles were about 40 and 130 nm. *In vitro* studied of skin permeation in hairy guinea pig skin showed that 40 nm minoxidil nanoparticles possessed 1.5-fold higher accumulation in the epidermal layer and 1.7-fold higher accumulation in the receptor solution than 130 nm minoxidil nanoparticles.

In 2009, Balakrishnan *et al.* [41] prepared minoxidil niosomes from sorbitan monoester with cholesterol by thin film-hydration method. The new minoxidil niosomes prepared from sorbitan monoester and cholesterol at 1:1 molar ratio, showed the minoxidil entrap efficiency of up to 60%. The niosomes showed negatively charged of -30 mV with an average diameter of 214 ± 32 nm. The

entrapped minoxidil permeation in hairless mouse skin was compared with commercial minoxidil solution 5% (Minoxyl). The skin accumulation of niosomal formulation was significantly greater than that of commercial formulation (19.41% vs 0.48%).

In 2009, Mura *et al.* [44] investigated the influence of vesicle to enhance the skin penetration of minoxidil. The minoxidil carrier contained soy lecithin, dicetylphosphate and different three different enhancers; Labrasol (capryl-caproyl macrogol 8-glyceride), Transcutol (2-(2-ethoxyethoxy)ethanol) and Cineole. *In vitro* study showed that the obtained vesicles were able to delivery to the pig skin a higher amount of minoxidil than traditional liposome as a control. The amount of minoxidil delivered through the skin by a control, Labrasol Transcutol and cineole were 6, 20, 8 and 17%, respectively.

In 2010, Hasanovic *et al.* [45] prepared 1,2-dipalmitoyl-sn-glycero-3-phosphocholine (DPPC) liposomes by high-pressure homogenizer, coated with a cationic polymer, Eudragit EPO (EU) or chitosan (CS). The cationic polymers had a stabilizing effect and enhanced skin permeation compared to the control liposomes. The polymeric coated liposomes showed slightly increased particle size. Zeta potential significantly increased by the addition of two different cationic polymers from 88.2 to 95.7 and 97.1 for control DPPC, EU DPPC and CS DPPC, respectively. The skin permeation efficiency of minoxidil also increased 1.54-fold and 1.88-fold after 10 h for EU DPPC and CS DPPC, respectively.

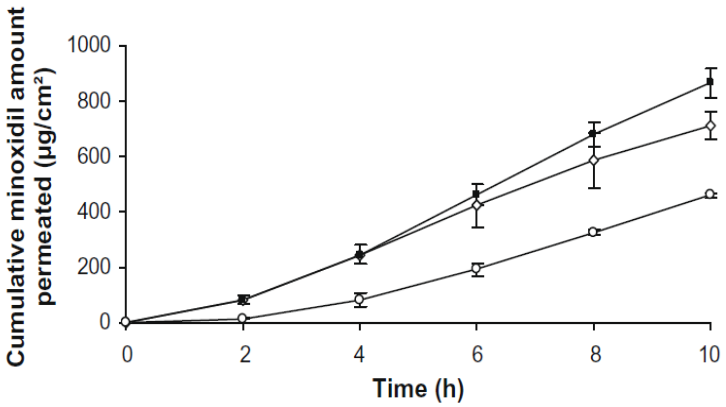

Figure 1.13 The skin permeation of minoxidil through porcine skin from different liposomal formulation: -■- EU-coated liposomes; -◇- CS-coated liposomes; -○- DPPC liposomes [45]

In 2011, Padois *et al.* [42] prepared solid lipid nanoparticles as minoxidil carrier without organic solvent and compared to commercial products. Solid lipid suspension contained semi-synthetic triglycerides, polysorbate, sorbitan oleate, minoxidil and water. The obtained mixture was homogenized by high pressure homogenizer at 40 °C. *Ex vivo* skin penetration in pig ear skin of the solid lipid nanoparticles suspension was as efficient as of the commercial products. *Ex vivo* skin corrosion study of solid lipid nanoparticles suspension has showed non-corrosive while commercial solutions presented a corrosive potential.

In 2013, Uprit *et al.* [46] prepared nanostructured lipid carrier (NLC) gel by melt dispersion ultrasonic method. The mixture of lipid and minoxidil was added into aqueous phase with Tween-80 (polysorbates 80) and continually stirred to form NLC suspension. The result showed high minoxidil encapsulation efficiency of 86.09%. The release profile studies of NLC showed prolong drug activity up to 16 h and displayed a biphasic drug release pattern with burst release at the initial stage followed by sustained release.

In 2014, Shatalebi *et al.* [47] developed and investigated a foamable emu oil emulsion containing minoxidil to improve skin permeation and hair growth. The foamable emulsion was prepared by mixing the oil phase with minoxidil solution using Tween 80 (polysorbates 80) as emulsifier. Hair growth potential of the prepared formulation exhibited higher numbers of hair follicles in anagenic phase than the commercial minoxidil solution (Pakdaru) and control group (96, 70 and 42%, respectively).

Figure 1.14 Albino rat skin treated with adopted formulation at day 20 (A) and at day 30 after the treatments (B). Commercial 5% minoxidil solution at day 20 (C) and at day 30 after the treatments (D). Blank formulation at day 20 (E) and at day 30 after the application (F). No drug as control group at day 20 (G) and at day 30 after application to the skin (H). [47]

Although liposomes and niosomes are alternative alcohol free minoxidil delivery systems, both vesicular systems are actually thermodynamic unstable, thus formulations of these vesicles possess limited half-life.

Schiff base is a carbon-nitrogen double bond (C=N) obtaining from condensation reaction of aldehyde or ketone compound reacting with primary amine to form imine bond. Schiff base is nitrogen analogues of aldehyde with C=N bond in

place of the carbonyl group (Figure 1.15). The Schiff bases have been widely used for several reasons. Schiff base can be conveniently form under mild condition and possesses strong coordinative ability, but is hydrolysable under acid condition [48]. In 2009, Jin *et al.* [49] studied the encapsulation of citral on chitosan by Schiff base reaction under high-intensity ultrasound. The success of Schiff base reaction showed a highest yield achieved was 86.4%, characterized by FTIR Spectroscopy. The result showed characteristic peak at 1648 cm^{-1} of C=N stretching confirming amino groups on chitosan coupled with citral via imine bond.

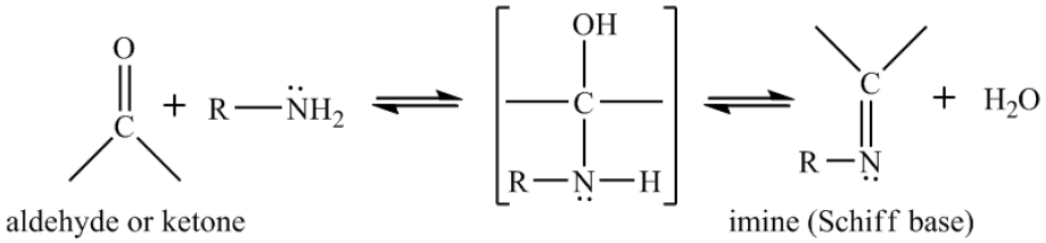

Figure 1.15 Schiff base formation [48]

1.7 Research goal

The objective of this research is to chemically modify cellulose in pineapple fiber waste into dialdehyde water soluble cellulose by periodate oxidation, and to use the obtained modified cellulose as a minoxidil carrier. The release profile of minoxidil, a drug model, from oxidized cellulose formulated nanoparticles will be studied under simulated human skin environment condition, pH 5.5 at 37°C.

The work project includes:

1. Preparation of dialdehyde water soluble cellulose via the Malaprade oxidation reaction.
2. Grafting minoxidil onto dialdehyde functionalized cellulose via Schiff base formation
3. Chemical structure, morphology and surface characterization of the obtaining cellulose nanoparticles
4. Controlled release study of minoxidil from the oxidized cellulose formulated nanoparticles

CHAPTER II

EXPERIMENTAL

2.1 Materials and Chemicals

Bleached pineapple fiber was provided by Tipco Group Public Company Limited (Bangkok, Thailand). Sodium metaperiodate and dialysis tubing cellulose membranes (MWCO 12,400 Da), size 76mm×49mm were purchased from Sigma-Aldrich (St. Louis, USA). Sodium thiosulfate and ethylene glycol were purchased from Carlo Erba (Milan, Italy). Potassium iodide was purchased from J.T.Baker (New Jersey, USA). Iodine was purchased from Fisher Chemical (Leicestershire, UK). Starch was purchased from Merck (Darmstadt, Germany). Minoxidil was obtained from Beta Pharma Company Limited (Shanghai, China). All solvents and chemicals were analytical grade and used without further purification.

2.2 Preparation of dialdehyde soluble cellulose

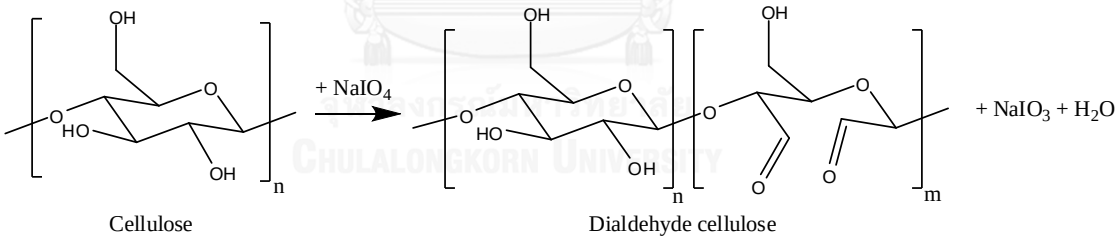

Figure 2.1 Synthesis of dialdehyde soluble cellulose

The synthesis of dialdehyde soluble cellulose was shown in Figure 2.1. Six hundred milligrams of bleached pineapple fiber was dispersed in 12 mL of deionized water and stirred for 2 hours at 55°C. Then, 8 mL of sodium metaperiodate, obtained by dissolving 586 mg of sodium metaperiodate in 8 mL of deionized water using sonicator to speed dissolution, was added (final concentration is 0.137 mol/L) to the dispersed suspension of cellulose and continued stirred in the dark at 55 °C for 3, 6,

15 and 24 hours, respectively. At the desired time, the reaction was quenched by the addition of excess ethylene glycol (500 µL) and stirred for 30 minutes at 55 °C. The reaction mixture was filtered and several times washed with deionized water to separate the insoluble pineapple fiber. The dialdehyde soluble cellulose was obtained as filtrate and was dialyzed against deionized water with gentle stirring to remove all leftover reagents. The insoluble fibers were dried in the oven (120 °C) overnight. The weight of dry insoluble fibers was used to calculate %yield of dialdehyde soluble cellulose using the following equation (1).

$$\% \text{ Yield } = \left(\frac{\text{Weight of initial pineapple fiber} - \text{Weight of precipitate}}{\text{Weight of initial pineapple fiber}}\right) \times 100 \quad (1)$$

The obtained dialdehyde soluble cellulose was dried using Freeze-Dry/Shell Freeze System model 7753501 (Labconco Corporation, Kansus, MI, USA) and characterized by Attenuated total reflectance-Fourier transform infrared (ATR-FTIR) (Thermo Electron Corporation, Madison, WI, USA), X-ray diffraction (XRD) (Rigaku International Corporation, Tokyo, Japan), scanning electron microscope (SEM) were used for morphological analysis (JEOL, Tokyo, Japan). Molecular weight (M_W) of dialdehyde soluble cellulose was determined by gel permeation chromatography (GPC) (Shimadzu, Kyoto, Japan). The size and zeta potential of particles were measured by dynamic light scattering technique (DLS) technique using a Zetasizer nanoseries (Malvern Instruments, Worcestershire, UK).

The leftover sodium metaperiodate was quantified (before added ethylene glycol) by UV Optizen Pop UV/Vis spectrophotometer (Mecasys Corporation, Daejeon, Korea) at 222 nm using a quartz cell 1 cm path-length operating at 25 °C. Calibration curve was created from a series of sodium metaperiodate solutions freshly prepared in deionized water at concentrations of 1, 3, 5, 10, 15 and 20 ppm (see calibration curve in appendix B). The experiment was repeated three times.

The content of aldehyde groups on dialdehyde soluble cellulose was determined by iodometric titration. Dialdehyde soluble cellulose solution at ~0.1 %

w/v (10 mL) was added to 20 mL of 0.025 M of I_2 solution, followed by the addition of 20 mL of 1.0 M of NaOH solution. The oxidation reaction proceeded for 15 minutes at room temperature and 15 mL of 6.25 % v/v of H_2SO_4 was added successively. The I_2 consumption by the reaction with aldehyde was determined by titration with 0.031 M of $Na_2S_2O_3$ using a few drops of starch solution as an indicator. The experiment was repeated three times. Noted that I_2 solution was prepared by dissolved 83g of KI in 800-900 mL of deionized water, added I_2 6.345 g and continued stirred until I_2 was dissolved. Adjust the volume to 1000 mL by deionized water (final concentration is 0.025 mole/L)

Oxidized soluble cellulose: ATR-FTIR (cm^{-1}): 3325 (O-H stretching vibration), 2927 and 2855 (C-H stretching vibration of aldehyde group), 1730 and 902 (C=O stretching of aldehyde group), 1025 (C-O-C stretching vibration).

2.3 Preparation of minoxidil-grafted dialdehyde soluble cellulose

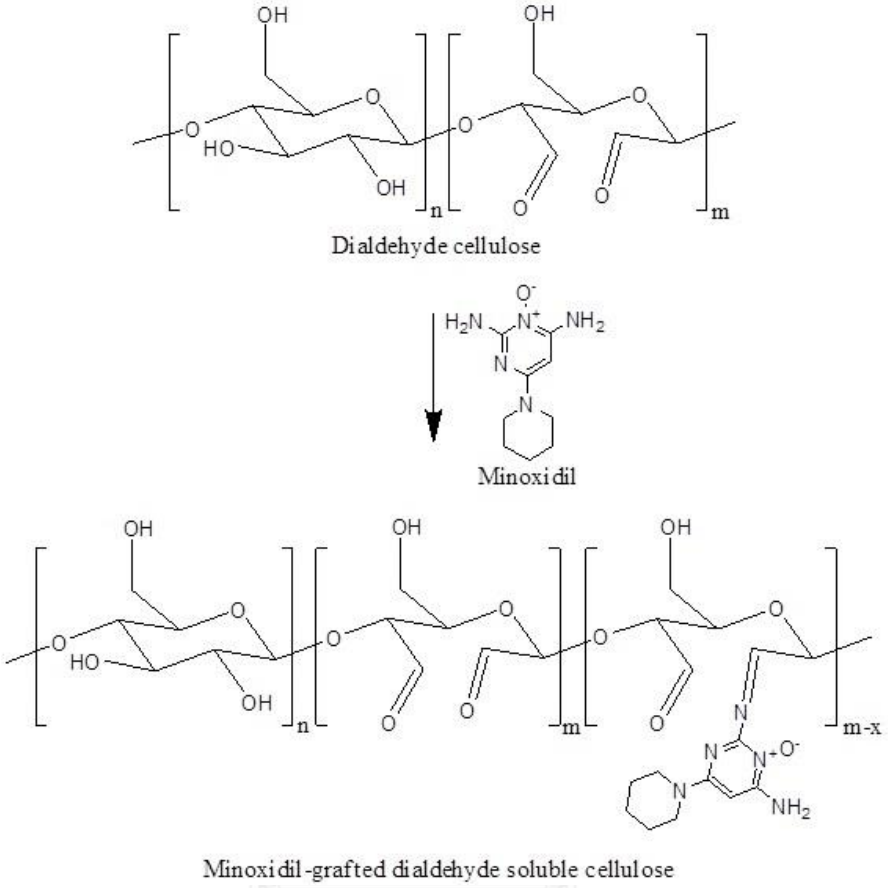

Figure 2.2 Synthesis of dialdehyde soluble cellulose

The dialdehyde soluble cellulose solution (0.2% w/v, 5mL) in deionized water from 2.2 was mixed with 3 mL of minoxidil solution (0.33 – 3.33% w/v) in ethanol in the different weight ratios of dialdehyde soluble cellulose to minoxidil (0:3, 1:1, 1:3, 1:5, 1:6, 1:7 and 1:8) under sonication (40 KHz, 30 °C) (see Table 2.). The mixture was continuously sonicated for 4 hours [50]. Ethanol in the mixture solution was slowly removed to give the final volume of 5 mL of aqueous phase by heating at 85 °C.

Table 2.1 Minoxidil-grafted dialdehyde soluble cellulose ratios.

Ratio of polymer : drug	Weight of dialdehyde soluble fiber in DI water 5 ml (mg)	Weight of minoxidil in ethanol 3 ml (mg)
0 : 3	0	30
1 : 1	10	10
1 : 3	10	30
1 : 5	10	50
1 : 6	10	60
1 : 7	10	70
1 : 8	10	80

2.4 Characterization of minoxidil-grafted dialdehyde soluble cellulose

2.4.1 Morphology of nanoparticles

Morphology of minoxidil-grafted dialdehyde soluble cellulose particles was characterized using attenuated total reflectance-Fourier transform infrared (ATR-FTIR), scanning electron microscopy (SEM) and transmission electron microscopy (TEM). The size and zeta potential of particles were measured by dynamic light scattering technique (DLS) using a Zetasizer nanoseries. Minoxidil-grafted dialdehyde soluble cellulose particles were also subjected to thermal gravimetric analysis (TGA).

2.4.1.1 Attenuated total reflectance-Fourier transform infrared (ATR-FTIR)

ATR-FTIR spectra were obtained using Nicolet 6700 FT-IR spectrometer (Thermo Electron Corporation, Madison, WI, USA) and ATR accessory consisting of a slide-on miniature germanium (Ge) as the internal reflection element was used, collecting with 64 scans in the mid-infrared region (4000 – 650 cm^{-1}): 3450 and 3407 cm^{-1} (N-H stretching vibration of NH_2 group), 1550 cm^{-1} (N-H bending vibration of NH_2 group), 1250 cm^{-1} (N-O stretching vibration) and 1222 cm^{-1} (C-N stretching vibration).

2.4.1.2 Scanning electron microscopic analysis (SEM)

SEM was performed by the Center for Analytical Service, Faculty of Science, Chulalongkorn University, Thailand. A drop of the nanoparticles suspension was placed on a glass slide and dried overnight. The sample was coated with a gold layer under vacuum at 15 mA for 90 s. The coated sample was then mounted on an SEM stud for visualization. The accelerating voltage used was 15 kV. The SEM photographs of minoxidil-grafted dialdehyde soluble cellulose nanoparticles were obtained using JSM-6610LV (JEOL, Ltd., Japan).

2.4.1.3 Transmission electron microscopic analysis (TEM)

TEM was performed by the Scientific and Technological Research Equipment Center, Chulalongkorn University, Thailand. TEM photographs were obtained using JEM-2100 (JEOL, Ltd., Japan) with an accelerating voltage of 120 kV in conjunction with selected area electron diffraction (SAED). A glass slide was dipped into the obtained suspension to gain the dried smooth film of nanoparticles on surface of the glass slide.

2.4.1.4 Dynamic light scattering technique (DLS)

The size and zeta potential of particles were measured by DLS using a Zetasizer nanoseries S4700 (Mulvern Instruments, Worcestershire, UK) equipped with a He–Ne laser beam at 632.8 nm (scattering angle of 173°). Each measurement was carried out in triplicate and an average value was reported. This analysis was carried out at Welltech Biotechnology (Lab) Co., Ltd. (Samut Sakhon, Thailand).

2.4.1.5 Thermal gravimetric analysis (TGA)

TGA was performed by the Scientific and Technological Research Equipment Center, Chulalongkorn University, Thailand using a Netzsch TG 209F3 Tarsus. Ten milligrams of the dry samples were precisely weighed into aluminium oxide pan. The experiments were performed under nitrogen with a scanning rate of 10°C/min^{-1} from 30-700°C.

2.5 The release of minoxidil from Schiff base nanoparticles

Entrapment efficiency percentage (% EE) and loading percentage of the nanoparticles were determined as followed. The obtained suspension of minoxidil-grafted dialdehyde soluble cellulose (0.5 mL) was centrifugally filtered by centrifugal-filtering devices with MWCO of 10,000 (Merck Millipore) at 5,000 rpm for 10 min. The filtrated solution was determined for the amount of minoxidil by UV-Vis spectrophotometer at wavelength 289 nm with the aid of calibration curve. Calibration curve was created from a series of minoxidil solutions freshly prepared in deionized water at concentration 1, 2, 3, 5, 7, 10 and 15 ppm (see calibration curve in appendix F). The entrapment efficiency percentage and loading percentage were calculated according to the following equations (2) and (3):

% EE and % loading were calculated from the following equations:

$$\text{Encapsulation efficiency (\%)} = (A/B) \times 100 \quad (2)$$

$$\text{Loading (\%)} = [A/(A+C)] \times 100 \quad (3)$$

Whereas A is weight of encapsulated minoxidil = weight of minoxidil used - weight of minoxidil found in filtrated;

B is weight of minoxidil used;

C is weight of polymer used.

All measurements were made in triplicate for each batch and mean values ± standard deviations were reported.

2.6 The release of minoxidil from Schiff base nanoparticles

Eighty milligrams of minoxidil-grafted dialdehyde soluble cellulose nanoparticles in dried form were dissolved in 10 mL of Acetate buffer solution pH 5.5 as the release medium. The tested sample (10 mL) was put into the dialysis membrane bag (MWCO 12,400 Da) and placed into 1000 mL of release medium and kept at 37 ± 0.1 ℃ with continuous stirring (at 100 rpm). One and a half milliliters of release medium were withdrawn at predetermined time intervals (0, 0.5, 1, 2, 3, 4, 5, 6, and 24 hours) and the same volume of release medium (37 ℃) was replaced. The amount of released minoxidil in withdrawn release medium was evaluated using UV-Vis Spectrophotometer at 37±0.1℃ at 287 nm. Calibration curve was created from a series of minoxidil solutions freshly prepared in Acetate buffer solution pH5.5 at concentrations of 1, 3, 5, 7, 10 and 15 ppm (see calibration curve in appendix G). Three repetitions were performed for all samples. The percentage of released minoxidil was calculated with the following equation (4):

$$\% \text{ minoxidil release} = \frac{\text{Weight of encapsulated minoxidil in release medium}}{\text{Weight of encapsulated minoxidil}} \text{ x } 100 \qquad (4)$$

CHAPTER III
RESULTS AND DISCUSSION

3.1 Preparation and characterization of dialdehyde soluble cellulose

The dialdehyde soluble cellulose was prepared by Malaprade reaction using sodium metaperiodate as a highly specific reagent to cleave C-2 and C-3 in glucopyranose ring of cellulose into 2,3-dialdehyde cellulose [29]. The oxidization reaction of cellulose from pineapple waste fiber is shown in Figure 3.1.

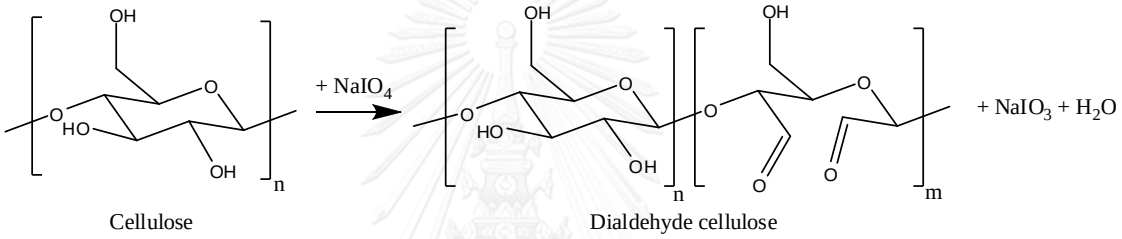

Figure 3.1 Synthesis of dialdehyde soluble cellulose

The oxidation reaction was carried out at different reaction times; 3, 6, 15 and 24 hours. The solution of oxidized cellulose became clearer when reaction time increased. To calculate percent yield of the oxidation process, defining as the amount of soluble fiber obtained from the originally water insoluble bleached fiber raw material, the precipitate of insoluble fiber were collected at different time intervals (3, 6, 15 and 24 hours) and dried in the oven before weighted. The percent yield of the process increased when the oxidation time increased. The percent yields at different reaction time (3, 6, 15 and 24 hours) were 23.30 ± 0.63, 45.74 ± 1.43, 66.68 ± 2.06 and 73.05 ± 1.39%, respectively (Figure 3.3). While the amount of sodium metaperiodate leftover in the solution before added ethylene glycol observed by UV absorption decreased significantly, especially during first 3h. During the oxidation reaction, the reaction should be kept in the dark place to avoid the

decomposition of periodate and photooxidation [31, 51]. The resulting aqueous dissolved and dried products are shown in Figure 3.2 (a) and (b), respectively. The physical appearance of the oxidized cellulose aqueous solution was pale yellow and transparent colloid dispersion. In case of dried-oxidized cellulose, the result showed pale yellow powder like needle or fiber. The dried product can be easily dissolved in water.

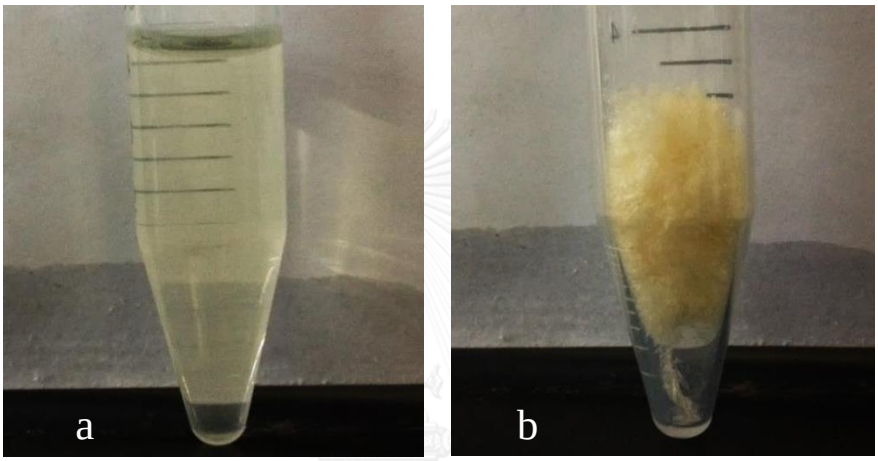

Figure 3.2 (a) The picture of dialdehyde soluble cellulose product in solution and (b) dry form

Figure 3.3 shows consumption of sodium metaperiodate, percent of aldehyde content determined by iodometric titration and molecular weight (Mw) examined by GPC at various reaction times. Although percent yield and the consumption of periodate indicated ongoing oxidation process, aldehyde content greatly decreased since the third hour onward. From previous studied suggested that the proceeding oxidation reaction of cellulose for long time is a self-acceleration process. When a glucopyranose ring on the polymer surface was converted to dialdehyde, the neighboring groups become more sensitive to oxidant due to loss of crystalline order [52]. This could possibly lead to the side reaction ; depolymerization [53]. Which was corresponding to a decrease of Mw resulting in higher amount of soluble cellulose. It

was possible that the break down soluble cellulose fibers were not oxidized into the dialdehyde as well as the oxidation of the originally soluble fibers, this might be a problem of too low concentration of periodate at later time. In fact, the low amounts of periodate found in the mixture corresponds well to this explanation. Therefore, the aldehyde content calculated based on mole of aldehyde to weight of soluble cellulose became lower when the reaction increased.

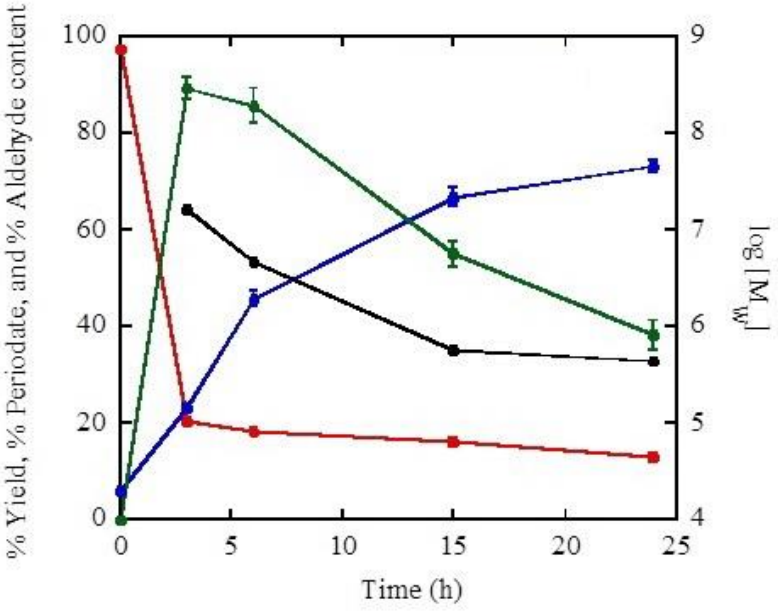

Figure 3.3 Percent yield (blue line), Percent of aldehyde content (green line) and molecular weight (black line) of dialdehyde soluble cellulose and Percent of leftover sodium metaperiodate (red line) in the reaction.

To characterize functional groups of dialdehyde soluble cellulose, the FT-IR spectroscopy was exploited. FT-IR spectra of cellulose fibers, before and after oxidization at various times, are shown in Figure 3.4. The IR spectra of dialdehyde soluble cellulose showed six characteristic peaks at 3325, 2927, 2855, 1730, 1024 and 902 cm^{-1}. Commonly, the absorbance at 3325 cm^{-1} referred to the O-H stretching from hydroxyl groups in cellulose structure. The absorption band at 2927 and 2855

cm^{-1} showed the C-H stretching from the aldehyde. The FTIR signal at 1024 cm^{-1} referred to the C-O-C stretching vibration of beta-1,4 glycosidic linkages. The absorption band at 902 cm^{-1} was assigned to the formation of hemiacetal bonds between the aldehyde groups and surrounded hydroxyl groups. The absorbance at 1730 cm^{-1}, a characteristic peak of C=O stretching in aldehyde groups increased corresponding to an increase of oxidation time. However, the 24 h product showed smaller 2855 cm^{-1} peak than the 15 h product. The 15 h product showed smaller 902 cm^{-1} peak than the 6 h product. This information agreed well with the above result which indicated less oxidation but more depolymerization and more yield at later time. Therefore, the FTIR spectra could confirm the presence of aldehyde groups in the oxidized fiber [54].

Therefore, we conclude that under the condition used here, the dialdehyde could be formed effectively during approximately the first 10 h, however, longer reaction time resulted in more soluble fibers.

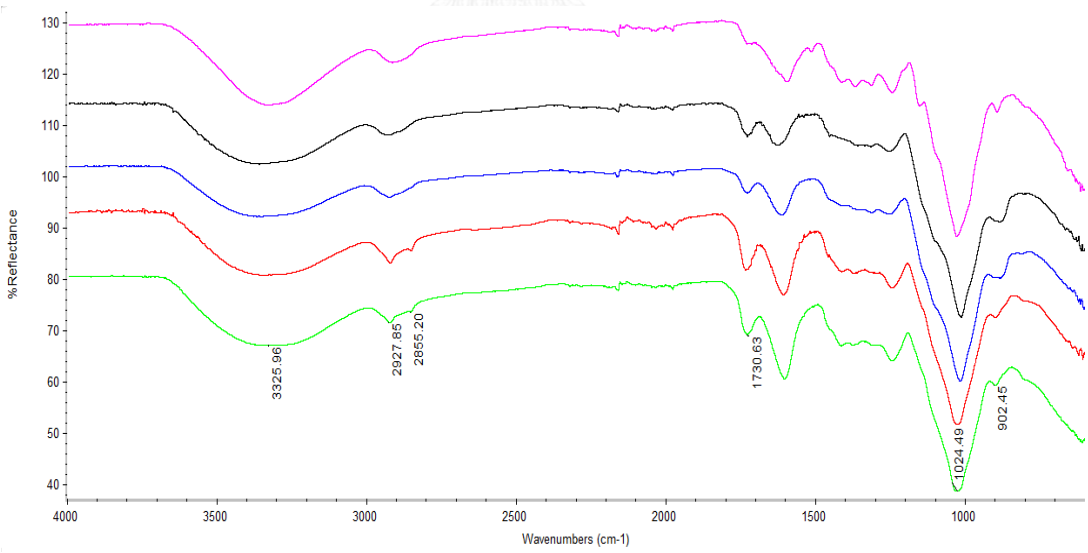

Figure 3.4 The ATR-FTIR spectrums of bleached pineapple fiber (pink line) and dialdehyde soluble cellulose at various times 3 h (black line), 6 h (blue line), 15 h (red line) and 24 h (green line)

The crystallographic structure of cellulose and dialdehyde soluble cellulose was determined using X-ray powder diffraction (XRD) analysis. The XRD diffractograms of cellulose exhibited peaks at 2θ of 22° [55] whereas that of dialdehyde soluble cellulose showed no peak. The disappearance of the peak at 2θ of 22° indicated decreased crystallization, changed ordered packing and destructed intermolecular hydrogen bonding from opening of glucopyranose rings (Figure 3.5) [52].

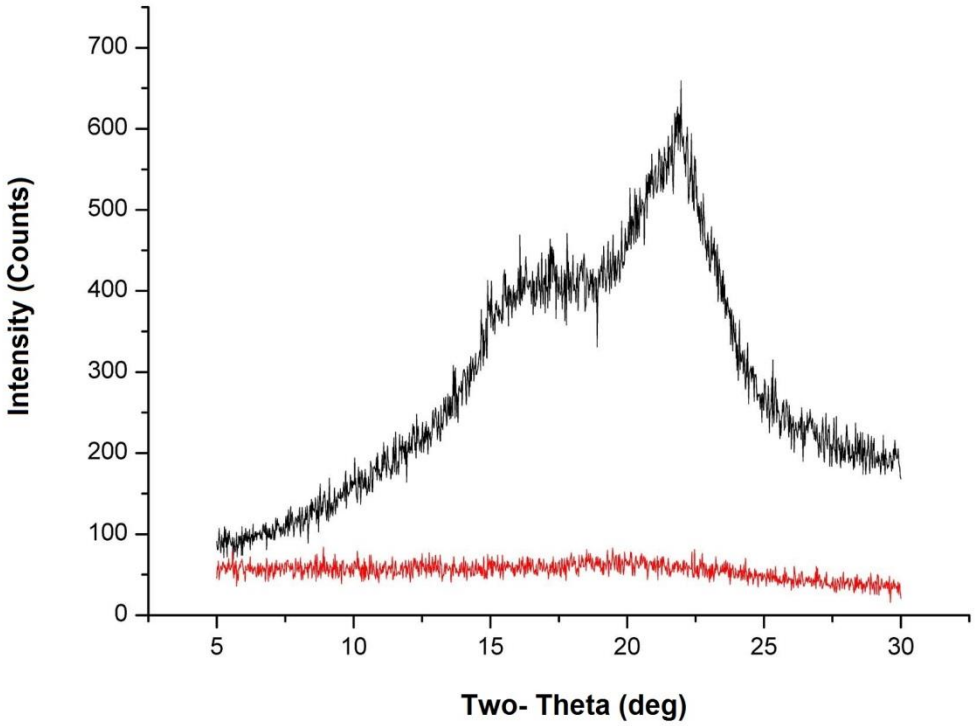

Figure 3.5 X-ray powder diffraction patterns of pineapple fiber (black line) and dialdehyde soluble cellulose (red line)

3.2 Preparation of minoxidil-grafted dialdehyde soluble cellulose

Here we used dialdehyde soluble cellulose as a carrier material, the minoxidil, a drug model, was grafted on the dialdehyde soluble cellulose to improve the water dispersability of minoxidil. The amino group on minoxidil could bond with aldehyde groups in dialdehyde soluble cellulose via a reversible Schiff's base formation. The mechanism of Schiff's base formation between minoxidil and dialdehyde soluble cellulose is shown in Figure 3.6.

Step 1: Acid catalyzed addition of amine to carbonyl

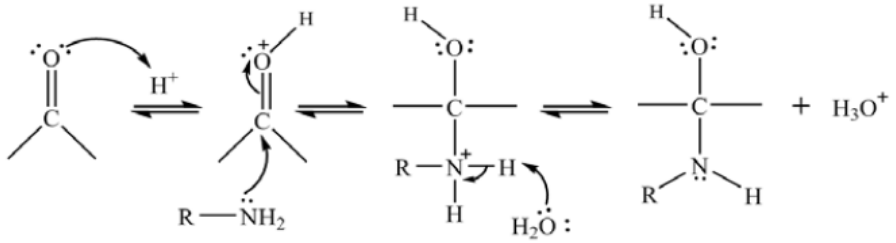

Step 2: Acid catalyzed dehydration

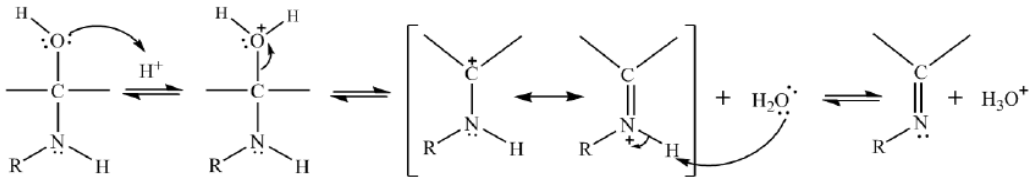

Figure 3.6 The mechanism of Schiff base formation [51]

Usually minoxidil precipitate quickly in water (2.2 mg/mL in water). However, when minoxidil was mixed with aqueous solution of the dialdehyde cellulose, the drug could be suspended. The minoxidil could be made suspendable in aqueous medium with no precipitation at dialdehyde soluble cellulose to minoxidil ratio of up to 1: 7 (wt/wt) (Table 3.1). The result showed that periodate-treated cellulose fiber at 15 hours exhibited the highest ability to make minoxidil suspendable in water with no precipitate. We speculate that the grafting through Schiff base was responsible for this dissolution of minoxidil. In addition, it was likely that during minoxidil-grafted dialdehyde soluble cellulose reaction, the self- assembly was also

taking place (see Figure 3.7 for the proposed model). The hydrophilic domains (hydroxyl group) of the cellulose arranged themselves to outer surface which interact with the hydrophilic water molecules. The hydrophobic domains including minoxidil arranged to core part. The optimal ratio 1: 7 between dialdehyde soluble cellulose and minoxidil also gave high %loading and %EE of 86.14 ± 0.03% and 88.75 ± 0.30%, respectively. At the obtained loading content of 1:7 of polymer to minoxidil weight ratio, it was speculated that both the grafted minoxidil moieties and the ungrafted minoxidil molecules were inside the particles (Figure 3.7). Since the aldehyde in the polymer can be estimated using iodometric titration to be 3.37×10^{-3} moles of aldehyde/gram of polymer (see appendix C) and 1 gram of minoxidil contains 4.78×10^{-3} moles of the material (estimated from molecular weight), at the weight ratio of 1:7 of polymer to minoxidil, the mole ratios of aldehyde to minoxidil is 1: 9.9. This indicates clearly that some minoxidil molecules are encapsulated in the particles without being chemically linked to the polymer via imine bond.

Table 3.1 Maximum amounts of minoxidil loading in various

Oxidizing time of dialdehyde soluble cellulose (hours)	Polymer : Minoxidil ratio (wt/wt)
3	1 : 0
6	1 : 4
15	1 : 7
24	1 : 5

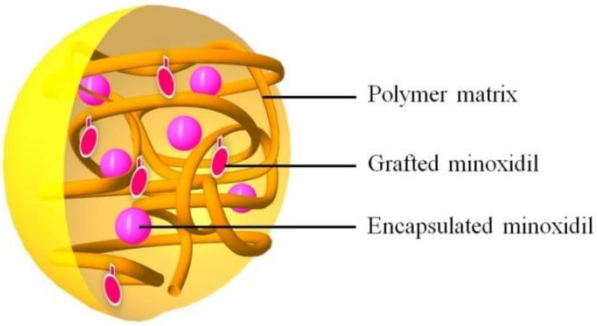

Figure 3.7 Schematic representation of minoxidil-grafted dialdehyde soluble cellulose nanoparticle

The minoxidil-grafted dialdehyde soluble cellulose particles showed good and stable dispersion in deionized water with no minoxidil precipitation. The physical appearance of minoxidil-grafted dialdehyde soluble cellulose particles in suspension was yellow with no aggregation (Figure 3.8 (a)). In case of dried dialdehyde soluble cellulose particles, the appearance was pale yellow powder (Figure 3.8 (b)). The obtained freeze-dried particle up to 1.4 %wt of minoxidil could be well redispersed in water.

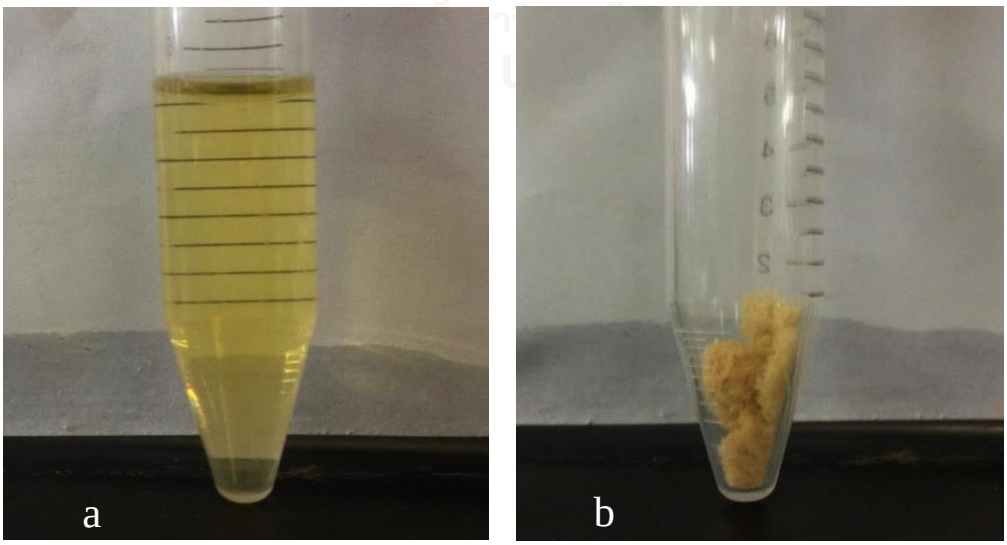

Figure 3.8 (a) minoxidil-grafted dialdehyde soluble cellulose solution and (b) dry product obtained at 1: 7 (wt/wt) of polymer: minoxidil ratio

3.3 Characterization of minoxidil-grafted dialdehyde soluble cellulose

The successful grafting of minoxidil moieties was confirmed by ATR-FTIR. ATR-FITR spectrum of minoxidil-grafted dialdehyde soluble cellulose (Figure 3.9 (green line)) showed a new characteristic peak at 1222 cm^{-1} corresponding to C-N stretching of tertiary amine. The characteristic peaks at 3450 and 3407 cm^{-1} of N-H stretching and 1550 cm^{-1} of N-H bending corresponded to the primary amine (NH_2) group of minoxidil were disappeared (Figure 3.9 (blue line)). This result confirmed that minoxidil moieties were successfully grafted on dialdehyde soluble cellulose via imine bond.

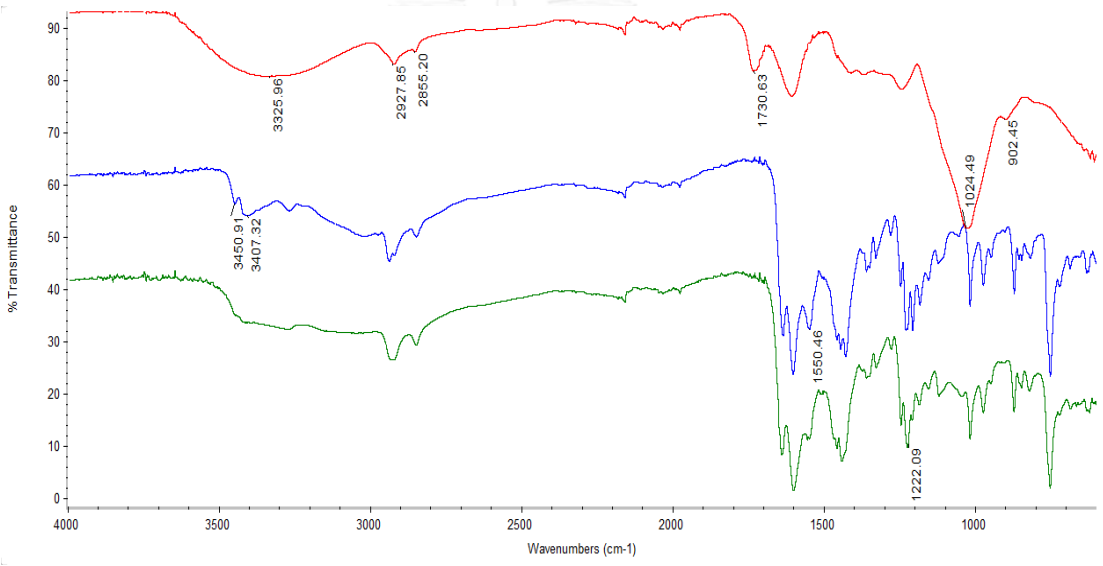

Figure 3.9 ATR-FTIR spectra of dialdehyde soluble cellulose (red line), minoxidil (blue line) and minoxidil-grafted dialdehyde soluble cellulose (green line)

Morphology of nanoparticles

The obtained nanoparticles in aqueous phase showed transparent suspension. The suspension of the sample was dried before being observed the morphology by SEM and TEM. SEM photographs showed the regular spherical particles in nanoscale size (140.0 ± 41.1 nm) and no aggregation of minoxidil (Figure

3.10 (a) and (b)). As shown in Figure 3.11 (a), the excess precipitate of minoxidil could be observed in samples at 8: 1(w/w) compared to unencapsulated minoxidil at 7: 0 (w/w) of drug to polymer ratio (Figure 3.11 (b)). The nanoparticles were also confirmed by TEM (Figure 3.12). The result showed the spherical shape without aggregation. And minoxidil could be in the core part of the particles.

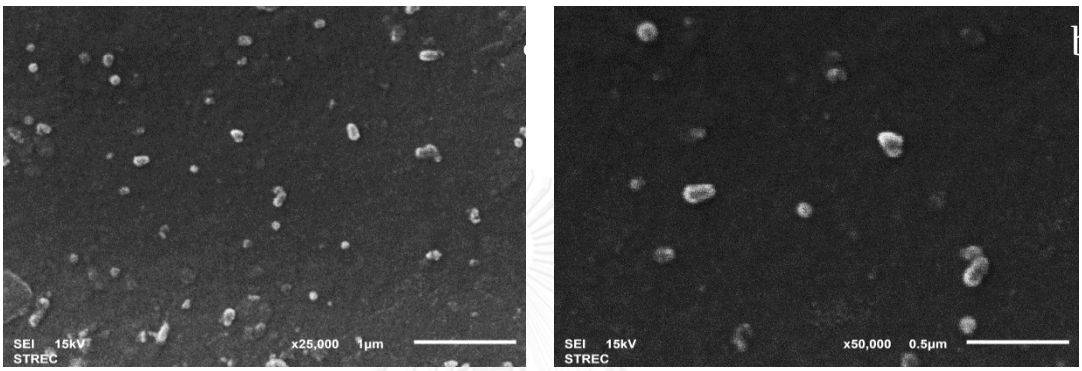

Figure 3.10 SEM photographs of minoxidil-grafted dialdehyde soluble cellulose nanoparticles at polymer concentration of 10 ppm (a) at 25,000x magnification and (b) at 50,000x magnification

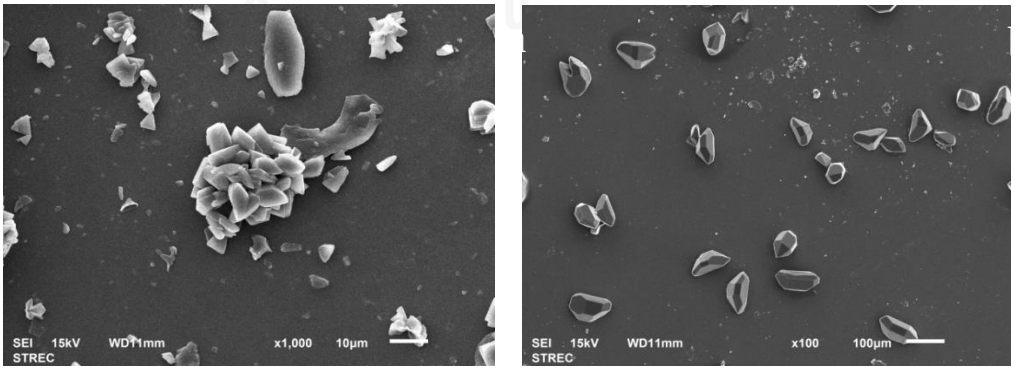

Figure 3.11 SEM photographs of (a) the excess precipitate of minoxidil in samples 8: 1 (w/w) of drug to polymer ratio and (b) unencapsulated minoxidil

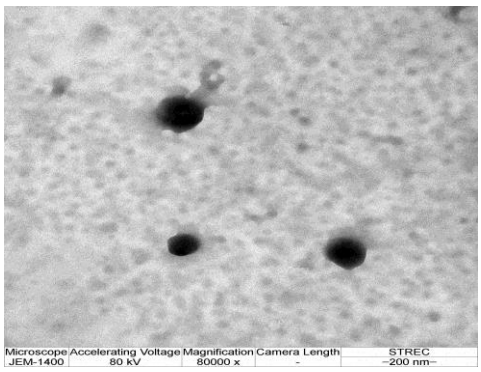

Figure 3.12 TEM photograph of minoxidil-grafted dialdehyde soluble cellulose nanoparticles at polymer concentration of 10 ppm

Size and surface charge of minoxidil-grafted dialdehyde soluble cellulose nanoparticles

To characterize particle size, the dynamic light scattering (DLS) was exploited. The sample suspension was freshly prepared. The hydrodynamic diameter, polydispersity index (PDI) and zeta potential value were obtained (Figure 3.13, 3.14). The results showed that diluted unloaded oxidized cellulose suspension gave a hydrodynamic diameter larger than minoxidil-grafted cellulose nanoparticles aqueous suspension, 521.1 ± 9.48 (PDI of 0.293) and 201.5 ± 11.65 nm (PDI of 0.263), respectively. Figure 3.13 showed size distribution spectrum of minoxidil-grafted cellulose nanoparticles measured by DLS, supporting the particle diameter ranged from 110 to 300 nm and corresponding to average size of 201 nm. This result indicated that after grafting minoxidil onto dialdehyde soluble cellulose, the polymer chains could rearrange to form the spheres and the grafted hydrophobic drug moieties then could be shielded from polar environment. This phenomenon resulted that the minoxidil-grafted cellulose nanoparticles decreased swelling comparing to the unloaded oxidized cellulose suspension. The zeta potential of oxidized cellulose and minoxidil-grafted cellulose nanoparticles were -15.6 ± 0.50 and -10.7 ± 0.09 mV, respectively (Figure 3.14). The negative surface charge of the nanoparticles supported

the conjecture that hydroxyl groups arranged themselves toward outer surface of the nanoparticles to interact with surrounding water molecules.

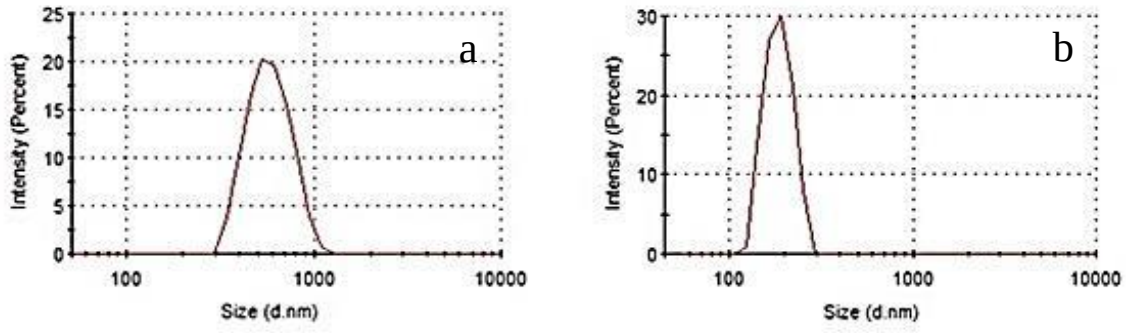

Figure 3.13 Size distributions of (a) unloaded particles and (b) minoxidil-grafted cellulose nanoparticles

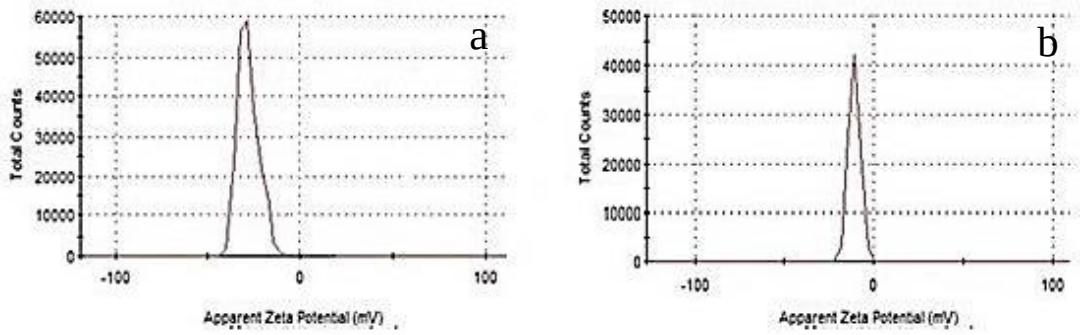

Figure 3.14 Zeta potential of (a) unloaded particles and (b) minoxidil-grafted cellulose nanoparticles

Form of minoxidil within polymeric nanoparticles

The interaction of minoxidil and polymer in the nanoparticles was investigated by thermal gravimetric analysis (TGA). TGA curve showed in Figure 3.15. The characteristic weight loss pattern of dialdehyde soluble cellulose and minoxidil observed at 221 and 286°C, respectively (Figure 3.15, 3.16) which corresponded to the degradation temperatures of dialdehyde soluble cellulose and minoxidil while the weight loss pattern at 221 and 286°C of minoxidil-grafted dialdehyde soluble cellulose was disappear. This indicates that there is no crystalline phase of minoxidil inside the particles. Moreover, the weight loss of minoxidil-grafted dialdehyde soluble cellulose was observed at 250°C. This shift of the weight loss pattern from 286.8°C observed in free minoxidil to 250°C in the minoxidil-loaded oxidized cellulose indicated that minoxidil interacted with dialdehyde soluble cellulose in nanoparticles.

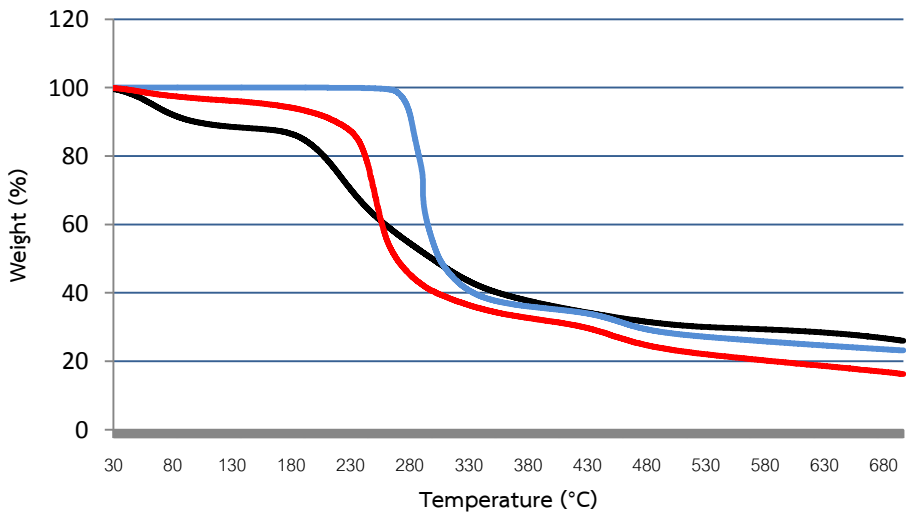

Figure 3.15 Thermo gravimetric analysis (TGA) curves of dialdehyde soluble cellulose (black line), minoxidil (blue line) and minoxidil-grafted cellulose nanoparticles (red line)

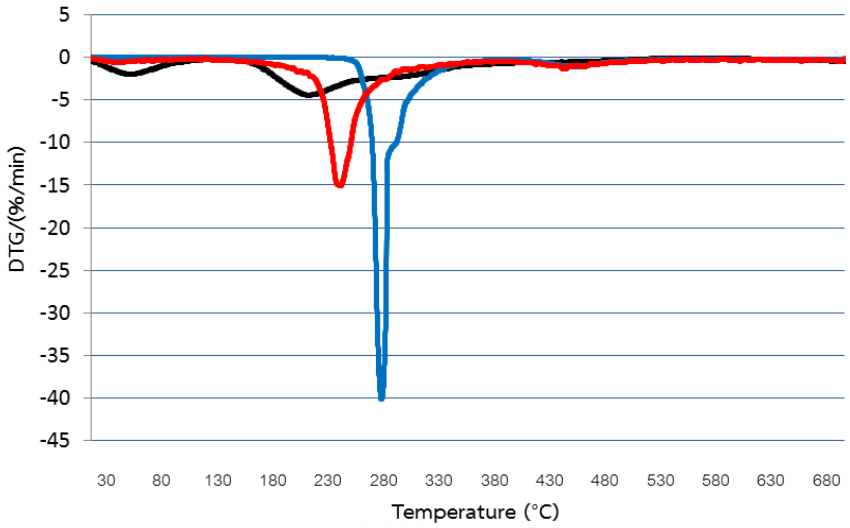

Figure 3.16 Derivative thermo gravimetric analysis (DTG) curves of dialdehyde soluble cellulose (black line), minoxidil (blue line) and minoxidil-grafted cellulose nanoparticles (red line)

3.4 Controlled release study of minoxidil

In this assay, we dissolved 80 mg of minoxidil-grafted dialdehyde soluble cellulose nanoparticles in 10 mL of acetate buffer pH 5.5 (the release medium). The obtained suspension was put into dialysis membrane bag and placed into 1000 mL of release medium with continuous stirring at 37 °C. One and a half milliliters of release medium were withdrawn at predetermined time intervals (0, 0.5, 1, 2, 3, 4, 5, 6, and 24 hours) and the same volume of release medium was replaced. The amount of released minoxidil in withdrawn release medium was evaluated using UV-Vis Spectrophotometer at 287 nm. Figure 3.17 showed the release profile of loaded minoxidil from the cellulose nanoparticles. This experiment was evaluated in acetate buffer solution pH 5.5 at 37 °C. This graph was plotted between percent release of minoxidil and release time

The result showed that the encapsulated minoxidil in nanoparticles was fast released into the release medium during the first hour. Diffusion of encapsulated minoxidil molecules inside nanoparticles seems to be concentration dependent

diffusion [56], since the rate of the release decreased with increasing time. It was likely that the concentration gradient between the inside and the outside of the particles decreased along the time. The amount of minoxidil released from nanoparticle was approximately 60% during the first 1-2 h. After that the grafted minoxidil molecules on the aldehyde functionalized cellulose fiber were probably hydrolyzed and gradually released from the nanoparticles, resulting in the sustained release of the rest of the minoxidil moieties. The accumulated percentages of released minoxidil from nanoparticle at 24 hours were 99.08%.

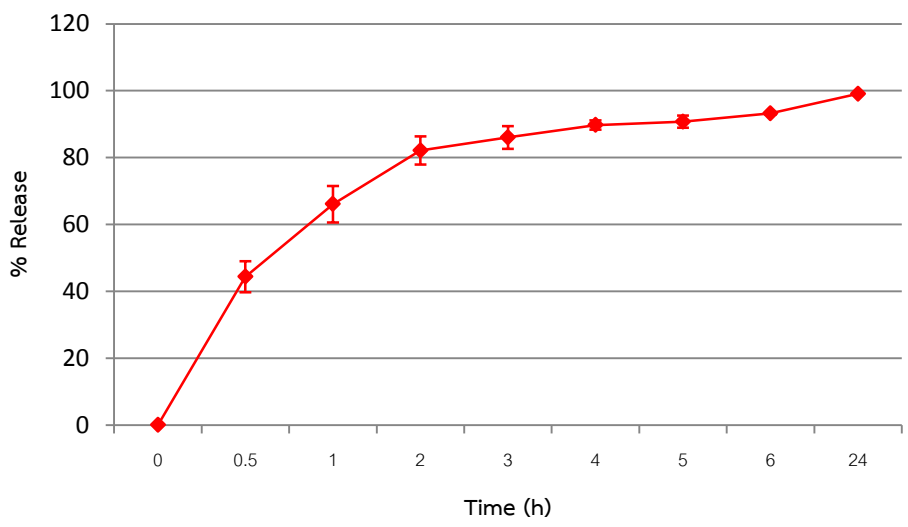

Figure 3.17 Release profile of minoxidil from the nanoparticles in acetate buffer solution (pH 5.5) at the indicated times (0, 0.5, 1, 2, 3, 4, 5, 6 and 24 hours)

CHAPTER IV
CONCLUSION

In this research, we have successfully synthesized minoxidil-grafted cellulose fiber from the bleached pineapple fiber waste. The obtained fiber could form nanoparticles and entrapped more minoxidil inside the particles. The optimized condition of oxidized cellulose was treated by sodium metaperiodate for 15 hours, 55°C. Minoxidil was successfully grafted onto dialdehyde soluble cellulose at 7 to 1 (w/w) of drug to polymer ratio using solvent removal process with high encapsulation efficiency (88.75%) and high loading capacity (86.14%). The obtained minoxidil-grafted dialdehyde soluble cellulose nanoparticles showed a spherical morphology with hydrodynamic diameter and negative surface charge of 201.5 ± 11.65 nm (PDI of 0.263) and -10.7 ± 0.09 mV, respectively. The nanoparticles, formed *via* self-assembling of polymer chains, displayed hydrophilic surface, dispersed well in water and non-organic solvent. The release profile of minoxidil from minoxidil-grafted dialdehyde soluble cellulose nanoparticles in acetate buffer solution pH 5.5, 37°C, indicated sustained release of minoxidil.

REFERENCES

[1] Plant protection research and development office; Department of Agriculture. Major pest of pineapple, situation and importance 2003: 40-41.

[2] granini.com. The Smooth Cayenne pineapple [internet]. [cited 2015 January 20]. Available from: http://www.granini.com/ww_en/spick-best-fruit/78/.

[3] Rohrbach, K.G., Leal, F., and d'Eeckenbrugge, G.C. History, distribution and world production. The pineapple: botany, production and uses. CABI, Honolulu (2002): 1-12.

[4] Levins, H. Social History of The Pineapple [internet]. [updated 2009; cited 2015 January 20]. Available from: http://www.levins.com/pineapple.html.

[5] Chaiwanichsiri, S., Laohasongkram, K., Thunpithayakul, C., and Mekmanee, S. Thermophysical properties of fresh and frozen pineapples. Asean Food Journal 11 (1996): 1-5.

[6] Food and Agriculture Organization of the United Nations (FAO). World pineapple production [internet]. [updated 2015; cited2015 January 20]. Available from: http://faostat3.fao.org/faostat-gateway/go/to/browse/Q/QC/E.

[7] Ketnawa, S., Chaiwut, P., and Rawdkuen, S. Pineapple wastes: A potential source for bromelain extraction. Food and bioproducts processing 90(3) (2012): 385-391.

[8] dos Santos, R.M., Neto, W.P.F., Silvério, H.A., Martins, D.F., Dantas, N.O., and Pasquini, D. Cellulose nanocrystals from pineapple leaf, a new approach for the reuse of this agro-waste. Industrial Crops and Products 50 (2013): 707-714.

[9] Zainuddin, M., Rosnah, S., Noriznan, M.M., and Dahlan, I. Effect of Moisture Content on Physical Properties of Animal Feed Pellets from Pineapple Plant Waste. Agriculture and Agricultural Science Procedia 2 (2014): 224-230.

[10] Kiran, E.U., Trzcinski, A.P., Ng, W.J., and Liu, Y. Bioconversion of food waste to energy: a review. Fuel 134 (2014): 389-399.

[11] Cherian, B.M., et al. Cellulose nanocomposites with nanofibres isolated from pineapple leaf fibers for medical applications. Carbohydrate Polymers 86(4) (2011): 1790-1798.

[12] Pardo, M.E.S., Cassellis, M.E.R., Escobedo, R.M., and García, E.J. Chemical Characterisation of the Industrial Residues of the Pineapple (Ananas comosus). Journal of Agricultural Chemistry and Environment 3(02) (2014): 53.

[13] Reis, C.P., Neufeld, R.J., Ribeiro, A.J., and Veiga, F. Nanoencapsulation I. Methods for preparation of drug-loaded polymeric nanoparticles. Nanomedicine: Nanotechnology, Biology and Medicine 2(1) (2006): 8-21.

[14] Couvreur, P., Dubernet, C., and Puisieux, F. Controlled drug delivery with nanoparticles: current possibilities and future trends. European journal of pharmaceutics and biopharmaceutics 41(1) (1995): 2-13.

[15] Christoforidis, J.B., Chang, S., Jiang, A., Wang, J., and Cebulla, C.M. Intravitreal devices for the treatment of vitreous inflammation. Mediators of inflammation 2012 (2012).

[16] de Souza Lima, M.M. and Borsali, R. Rodlike cellulose microcrystals: structure, properties, and applications. Macromolecular Rapid Communications 25(7) (2004): 771-787.

[17] Kamide, K. 2 - Characterization of Molecular Structure of Cellulose Derivatives. in Kamide, K. (ed.)Cellulose and Cellulose Derivatives, pp. 25-188. Amsterdam: Elsevier, 2005.

[18] Ross, P., Mayer, R., and Benziman, M. Cellulose biosynthesis and function in bacteria. Microbiological reviews 55(1) (1991): 35-58.

[19] Myasoedova, V.V. Physical chemistry of non-aqueous solutions of cellulose and its derivatives. (2000).

[20] Gross, R.A. and Scholz, C. Biopolymers from polysaccharides and agroproteins. (2001).

[21] Bochek, A. Effect of hydrogen bonding on cellulose solubility in aqueous and nonaqueous solvents. Russian journal of applied chemistry 76(11) (2003): 1711-1719.

[22] John, M.J. and Thomas, S. Biofibres and biocomposites. Carbohydrate Polymers 71(3) (2008): 343-364.

[23] Moon, R.J., Martini, A., Nairn, J., Simonsen, J., and Youngblood, J. Cellulose nanomaterials review: structure, properties and nanocomposites. Chemical Society Reviews 40(7) (2011): 3941-3994.

[24] Hinterstoisser, B. and Salmén, L. Application of dynamic 2D FTIR to cellulose. Vibrational Spectroscopy 22(1) (2000): 111-118.

[25] Nishiyama, Y. Structure and properties of the cellulose microfibril. Journal of wood science 55(4) (2009): 241-249.

[26] Singh, M., Ray, A.R., and Vasudevan, P. Biodegradation studies on periodate oxidized cellulose. Biomaterials 3(1) (1982): 16-20.

[27] sciencelab.com. Material Safety Data Sheet of Cellulose [internet]. [updated 2013; cited 2015 January 20]. Available from http://www.sciencelab.com/msds.php?msdsId=9927490.

[28] Hon, D.N.-S. and Shiraishi, N. Wood and Cellulosic Chemistry, Revised, and Expanded. CRC Press, 2000.

[29] Varma, A. and Kulkarni, M. Oxidation of cellulose under controlled conditions. Polymer Degradation and Stability 77(1) (2002): 25-27.

[30] Anjali, T. Modification of carboxymethyl cellulose through oxidation. Carbohydrate Polymers 87(1) (2012): 457-460.

[31] Hou, Q., Liu, W., Liu, Z., and Bai, L. Characteristics of wood cellulose fibers treated with periodate and bisulfite. Industrial & Engineering Chemistry Research 46(23) (2007): 7830-7837.

[32] Kristiansen, K.A., Potthast, A., and Christensen, B.E. Periodate oxidation of polysaccharides for modification of chemical and physical properties. Carbohydrate research 345(10) (2010): 1264-1271.

[33] Liu, X., Wang, L., Song, X., Song, H., Zhao, J.R., and Wang, S. A kinetic model for oxidative degradation of bagasse pulp fiber by sodium periodate. Carbohydrate Polymers 90(1) (2012): 218-223.

[34] Ashenhurst, J. Sodium Periodate. [internet]. [cited 2015 January 20]. Available from http://www.masterorganicchemistry.com/2011/10/21/reagent-friday-sodium-periodate/ (2011).

[35] Bouhadir, K.H., Lee, K.Y., Alsberg, E., Damm, K.L., Anderson, K.W., and Mooney, D.J. Degradation of partially oxidized alginate and its potential application for tissue engineering. Biotechnology progress 17(5) (2001): 945-950.

[36] Kanth, S.V., Ramaraj, A., Rao, J.R., and Nair, B.U. Stabilization of type I collagen using dialdehyde cellulose. Process Biochemistry 44(8) (2009): 869-874.

[37] Kristiansen, K.A., Tomren, H.B., and Christensen, B.E. Periodate oxidized alginates: Depolymerization kinetics. Carbohydrate Polymers 86(4) (2011): 1595-1601.

[38] Liimatainen, H., Visanko, M., Sirvio, J.A., Hormi, O.E., and Niinimaki, J. Enhancement of the nanofibrillation of wood cellulose through sequential periodate–chlorite oxidation. Biomacromolecules 13(5) (2012): 1592-1597.

[39] DuCHARME, D.W., FREYBURGER, W.A., GRAHAM, B.E., and CARLSON, R.G. Pharmacologic properties of minoxidil: a new hypotensive agent. Journal of Pharmacology and Experimental Therapeutics 184(3) (1973): 662-670.

[40] Kudlacek, P.E., Anderson, R.J., Liebentritt, D.K., Johnson, G.A., and Huerter, C.J. Human skin and platelet minoxidil sulfotransferase activities: biochemical properties, correlations and contribution of thermolabile phenol sulfotransferase. Journal of Pharmacology and Experimental Therapeutics 273(2) (1995): 582-590.

[41] Balakrishnan, P., et al. Formulation and in vitro assessment of minoxidil niosomes for enhanced skin delivery. International journal of pharmaceutics 377(1) (2009): 1-8.

[42] Padois, K., Cantiéni, C., Bertholle, V., Bardel, C., Pirot, F., and Falson, F. Solid lipid nanoparticles suspension versus commercial solutions for dermal delivery of minoxidil. International journal of pharmaceutics 416(1) (2011): 300-304.

[43] Shim, J., Kang, H.S., Park, W.-S., Han, S.-H., Kim, J., and Chang, I.-S. Transdermal delivery of mixnoxidil with block copolymer nanoparticles. Journal of controlled release 97(3) (2004): 477-484.

[44] Mura, S., Manconi, M., Sinico, C., Valenti, D., and Fadda, A.M. Penetration enhancer-containing vesicles (PEVs) as carriers for cutaneous delivery of minoxidil. International journal of pharmaceutics 380(1) (2009): 72-79.

[45] Hasanovic, A., Hollick, C., Fischinger, K., and Valenta, C. Improvement in physicochemical parameters of DPPC liposomes and increase in skin permeation of aciclovir and minoxidil by the addition of cationic polymers. European journal of pharmaceutics and biopharmaceutics 75(2) (2010): 148-153.

[46] Uprit, S., Sahu, R.K., Roy, A., and Pare, A. Preparation and characterization of minoxidil loaded nanostructured lipid carrier gel for effective treatment of alopecia. Saudi Pharmaceutical Journal 21(4) (2013): 379-385.

[47] Shatalebi, Y.R. Preparation and evaluation of minoxidil foamable emu oil emulsion. Research in Pharmaceutical Sciences 9(2) (2013): 123-133.

[48] Wade Jr, L. Organic-chemistry. sixth edition. 2008, Upper Saddle River, New Jersey: Pearson Prentice Hall.

[49] Jin, X., Wang, J., and Bai, J. Synthesis and antimicrobial activity of the Schiff base from chitosan and citral. Carbohydrate research 344(6) (2009): 825-829.

[50] Tree-udom, T., Wanichwecharungruang, S.P., Seemork, J., and Arayachukeat, S. Fragrant chitosan nanospheres: Controlled release systems with physical and chemical barriers. Carbohydrate Polymers 86(4) (2011): 1602-1609.

[51] Sirvio, J., Hyvakko, U., Liimatainen, H., Niinimaki, J., and Hormi, O. Periodate oxidation of cellulose at elevated temperatures using metal salts as cellulose activators. Carbohydrate Polymers 83(3) (2011): 1293-1297.

[52] Kim, U.-J., Kuga, S., Wada, M., Okano, T., and Kondo, T. Periodate oxidation of crystalline cellulose. Biomacromolecules 1(3) (2000): 488-492.

[53] Vold, I.M. and Christensen, B.E. Periodate oxidation of chitosans with different chemical compositions. Carbohydrate research 340(4) (2005): 679-684.

[54] Mu, C., Guo, J., Li, X., Lin, W., and Li, D. Preparation and properties of dialdehyde carboxymethyl cellulose crosslinked gelatin edible films. Food Hydrocolloids 27(1) (2012): 22-29.

[55] Varma, A., Jamdade, Y., and Nadkarni, V. Wide-angle X-ray diffraction study of the effect of periodate oxidation and thermal treatment on the structure of cellulose powder. Polymer Degradation and Stability 13(1) (1985): 91-98.

[56] Lee, J.H. and Yeo, Y. Controlled drug release from pharmaceutical nanocarriers. Chemical Engineering Science (2014).

APPENDIX

APPENDIX A

1. Calculation of % yield of dialdehyde soluble cellulose

$$\%\ \text{Yield} = \left(\frac{\text{Weight of initial pineapple fiber} - \text{Weight of precipitate}}{\text{Weight of initial pineapple fiber}}\right) \times 100$$

- % yield at 0 h

Weight of initial pineapple fiber = 600.20 mg

Weight of precipitate = 559.93 mg

$$\%\ \text{yield} = \left(\frac{600.20 - 559.93}{600.20}\right) \times 100$$

= 6.71 %

- % yield at 3 h

Weight of initial pineapple fiber = 600.40 mg

Weight of precipitate = 464.27 mg

$$\%\ \text{yield} = \left(\frac{600.40 - 464.27}{600.40}\right) \times 100$$

= 22.69 %

- % yield at 6 h

Weight of initial pineapple fiber = 600.00 mg

Weight of precipitate = 324.27 mg

$$\%\ \text{yield} = \left(\frac{600.00 - 324.27}{600.00}\right) \times 100$$

= 45.96 %

- % yield at 15 h

Weight of initial pineapple fiber = 600.20 mg

Weight of precipitate = 199.26 mg

$$\% \text{ yield} = \left(\frac{600.20 - 199.26}{600.20}\right) \times 100$$

= 66.82 %

- % yield at 24 h

Weight of initial pineapple fiber = 600.30 mg

Weight of precipitate = 157.40 mg

$$\% \text{ yield} = \left(\frac{600.30 - 157.40}{600.30}\right) \times 100$$

= 73.82 %

APPENDIX B

1. Calculation of % sodium metaperiodate in the reaction

The calibration curve of sodium metaperiodate was prepared using sodium metaperiodate solution in deionized water at concentration 0, 1, 3, 5, 10, 15 and 20 ppm. A calibration curve was plotted between each sodium metaperiodate concentration and its corresponding absorbance value as shown in Table B1 and Figure B1. The concentration of sodium metaperiodate in the reaction was determined by comparison to this calibration curve.

Table B1 sodium metaperiodate concentration and its corresponding absorbance value at 222 nm

Concentration (ppm)	**0**	**1**	**3**	**5**	**10**	**15**	**20**
Absorbance at 320 nm	0.000	0.049	0.147	0.271	0.482	0.747	0.946

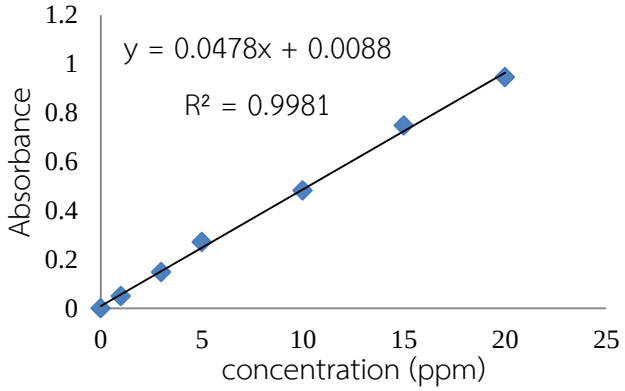

Figure B1 Calibration curve of sodium metaperiodate at 222 nm

By plotting a graph between absorbance and concentrations of standard sodium metaperiodate solutions, a linear relationship was obtained and used for calculation of concentration of sodium metaperiodate.

From the equation of calibration curve;

$$Y = 0.0478X + 0.0088,\ R^2 = 0.9981 \qquad (1)$$

1.1 Calculation % sodium metaperiodate in the reaction

- Sodium metaperiodate remaining in the reaction at 0 h

From equation (1) $Y = 0.0478X + 0.0088$

$0.961 = 0.0478X + 0 .0088$

$X = 20.27$

Dilution factor = 1470 $X = 20.27 \times 1470$

$X = 29800$ ppm

Weight of sodium metaperiodate in 20 mL = 29800×0.02

= 585.7 ppm

% periodate remaining at 0 hour: periodate initial used = 586.3 mg

periodate found in reaction = 585.7 mg

% periodate remaining = (585.7/586.3) x 100

= 99.94 %

- Sodium metaperiodate remaining in the reaction at 3 h

From equation (1) $Y = 0.0478X + 0.0088$

$0.205 = 0.0478X + 0 .0088$

$X = 4.10$

Dilution factor = 1470 $X = 4.10 \times 1470$

$X = 6034$ ppm

Weight of sodium metaperiodate in 20 mL = 6034×0.02

= 120.7 ppm

% periodate remaining at 3 hour: periodate initial used = 586.3 mg

periodate found in reaction = 120.7 mg

% periodate remaining = (120.7/586.3) x 100

= 20.58 %

- Sodium metaperiodate remaining in the reaction at 6 h

From equation (1) Y = 0.0478X + 0.0088

0.186 = 0.0478X + 0 .0088

X = 3.71

Dilution factor = 1470 X = 3.71 x 1470

X = 5449 ppm

Weight of sodium metaperiodate in 20 mL = 5449 x 0.02

= 108.9 ppm

% periodate remaining at 6 hour: periodate initial used = 586.3 mg

periodate found in reaction = 108.9 mg

% periodate remaining = (108.9/586.3) x 100

= 18.59 %

- Sodium metaperiodate remaining in the reaction at 15 h

From equation (1) Y = 0.0478X + 0.0088

0.163 = 0.0478X + 0 .0088

X = 3.23

Dilution factor = 1470 X = 3.23 x 1470

X = 4742 ppm

Weight of sodium metaperiodate in 20 mL = 4742 x 0.02

= 94.8 ppm

% periodate remaining at 15 hour: periodate initial used = 586.3 mg

periodate found in reaction = 94.8 mg

% periodate remaining = (94.8/586.3) x 100

= 16.18 %

- Sodium metaperiodate remaining in the reaction at 24 h

From equation (1) Y = 0.0478X + 0.0088

0.133 = 0.0478X + 0 .0088

X = 2.59

Dilution factor = 1470 X = 2.59 x 1470

X = 3819 ppm

Weight of sodium metaperiodate in 20 mL = 3819 x 0.02

= 76.4 ppm

% periodate remaining at 24 hour: periodate initial used = 586.3 mg

periodate found in reaction = 76.4 mg

% periodate remaining = (76.4/586.3) x 100

= 13.03 %

APPENDIX C

1. Calculation of % aldehyde content in the dialdehyde soluble cellulose

$$\text{Mole of aldehyde} = \left(\frac{\text{C Iodine} \times (\text{V Blank} - \text{V Sample})}{1000}\right) \times \frac{\text{C Iodine}}{\text{C Sodium thiosulfate}}$$

Where,

C_{Iodine} = concentration of iodine = 0.025 mole/L

$C_{Sodium\ thiosulfate}$ = concentration of sodium thiosulfate = 0.031 mole/L

V_{Blank} = volume of sodium thiosulfate in blank

V_{Sample} = volume of sodium thiosulfate in sample

$$\%\ \text{Aldehyde content} = \left(\frac{\text{Mole of aldehyde}}{\left(\frac{\text{W Sample}}{\text{Mw of cellulose}}\right)}\right) \times 100$$

Where,

W_{sample} = weighed amount of sample (g)

$M_{w\ of\ cellulose}$ = 164.24 g/mole

- % aldehyde content in the dialdehyde soluble cellulose at 0 h

V_{Blank} = 29.67 mL

V_{Sample} = 27.50 mL

$$\text{Mole of aldehyde} = \left(\frac{0.025 \times (29.67 - 27.50)}{1000}\right) \times \frac{0.025}{0.031}$$

$$= 4.375 \times 10^{-5}\ mole$$

$$\%\ \text{Aldehyde content} = \left(\frac{4.375 \times 10^{-5}}{\left(\frac{0.1000}{164.24}\right)}\right) \times 100$$

$$= 7.09\ \%$$

- % aldehyde content in the dialdehyde soluble cellulose at 3 h

V_{Blank} = 29.67 mL

V_{Sample} = 1.95 mL

$$\text{Mole of aldehyde} = \left(\frac{0.025 \times (29.67 - 1.95)}{1000}\right) \times \frac{0.025}{0.031}$$

$$= 5.589 \times 10^{-4}\ mole$$

$$\%\ \text{Aldehyde content} = \left(\frac{5.589 \times 10^{-4}}{\left(\frac{0.1024}{164.24}\right)}\right) \times 100$$

$$= 88.49\ \%$$

- % aldehyde content in the dialdehyde soluble cellulose at 6 h

V_{Blank} = 29.67 mL

V_{Sample} = 4.29 mL

$$\text{Mole of aldehyde} = \left(\frac{0.025 \times (29.67 - 4.29)}{1000}\right) \times \frac{0.025}{0.031}$$

$$= 5.117 \times 10^{-4}\ mole$$

$$\%\ \text{Aldehyde content} = \left(\frac{5.117 \times 10^{-4}}{\left(\frac{0.1027}{164.24}\right)}\right) \times 100$$

$$= 80.78\ \%$$

- % aldehyde content in the dialdehyde soluble cellulose at 15 h

$V_{Blank} = 29.67$ mL

$V_{Sample} = 12.76$ mL

$$\text{Mole of aldehyde} = \left(\frac{0.025 \times (29.67 - 12.76)}{1000}\right) \times \frac{0.025}{0.031}$$

$$= 3.409 \times 10^{-4}\ mole$$

$$\%\ \text{Aldehyde content} = \left(\frac{3.409 \times 10^{-4}}{\left(\frac{0.1012}{164.24}\right)}\right) \times 100$$

$$= 54.62\ \%$$

- % aldehyde content in the dialdehyde soluble cellulose at 24 h

$V_{Blank} = 29.67$ mL

$V_{Sample} = 17.54$ mL

$$\text{Mole of aldehyde} = \left(\frac{0.025 \times (29.67 - 17.54)}{1000}\right) \times \frac{0.025}{0.031}$$

$$= 2.446 \times 10^{-4}\ mole$$

$$\%\ \text{Aldehyde content} = \left(\frac{2.446 \times 10^{-4}}{\left(\frac{0.1028}{164.24}\right)}\right) \times 100$$

$$= 38.57\ \%$$

APPENDIX D

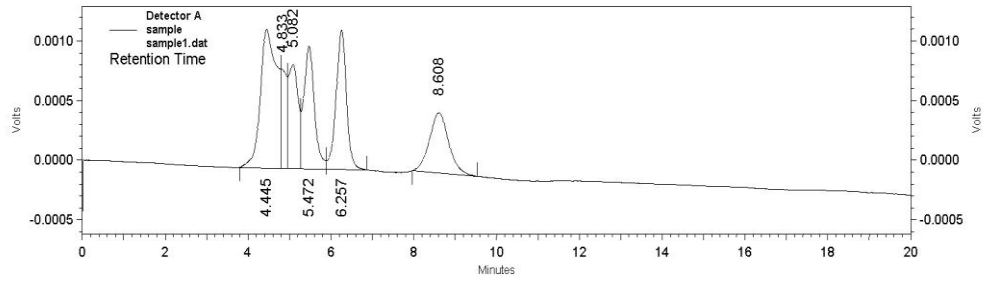

Figure D1 GPC chromatogram of dialdehyde soluble cellulose at 3 h

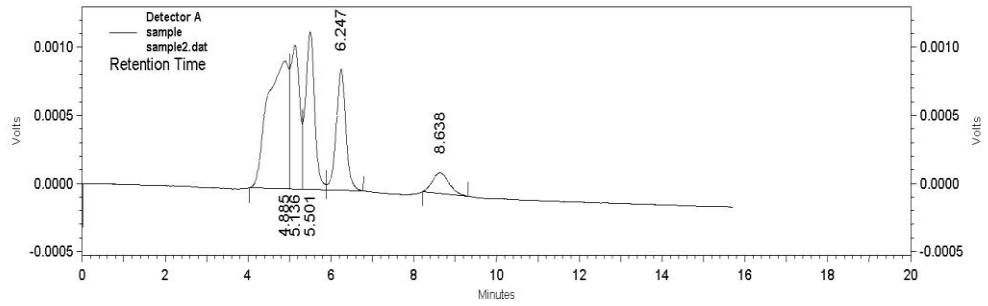

Figure D2 GPC chromatogram of dialdehyde soluble cellulose at 6 h

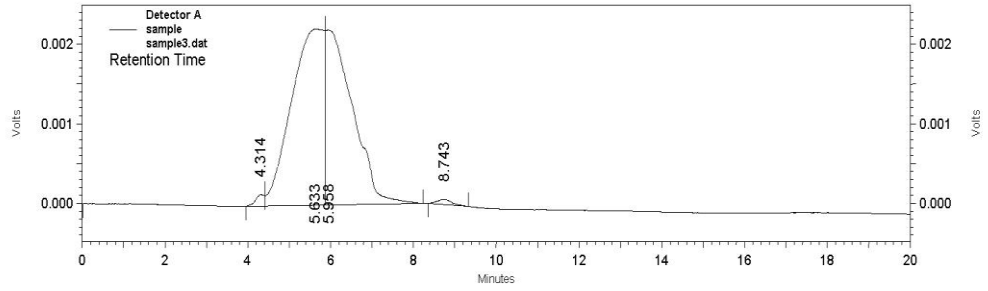

Figure D3 GPC chromatogram of dialdehyde soluble cellulose at 15 h

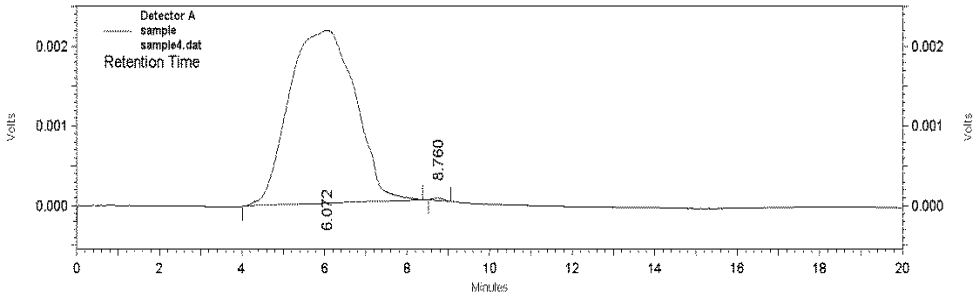

Figure D4 GPC chromatogram of dialdehyde soluble cellulose at 24 h

APPENDIX E

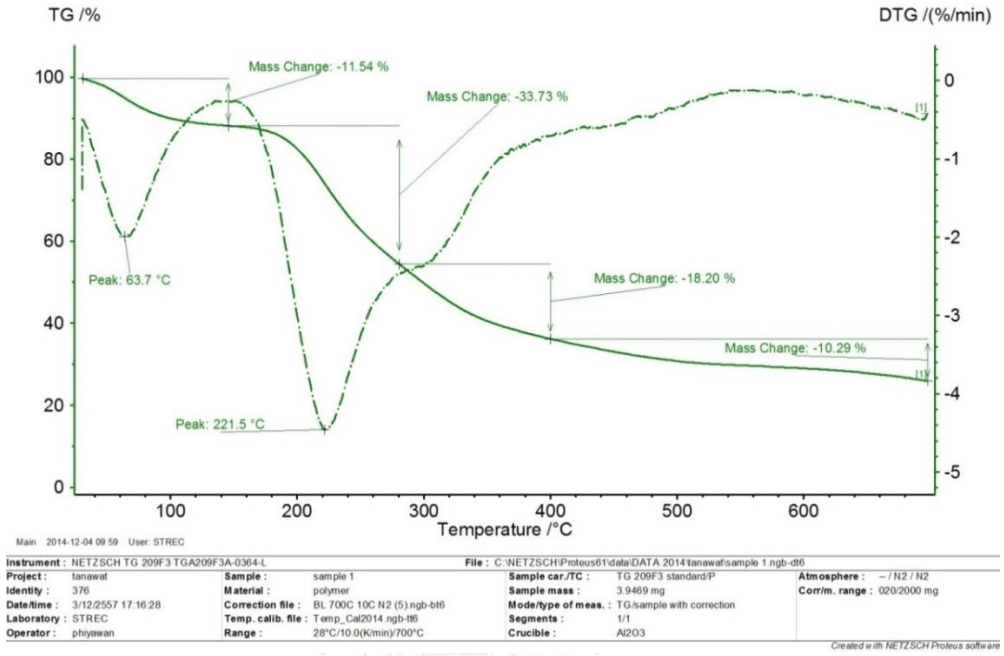

Figure E1 Thermo gravimetric analysis (TGA) curves of dialdehyde soluble cellulose

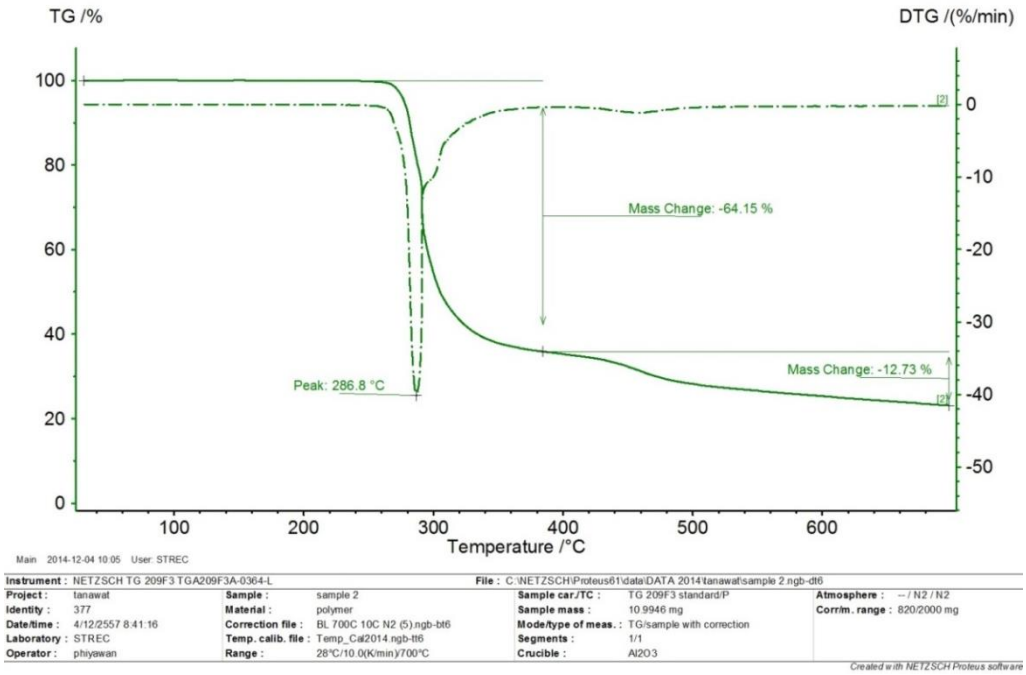

Figure E2 Thermo gravimetric analysis (TGA) curves of minoxidil

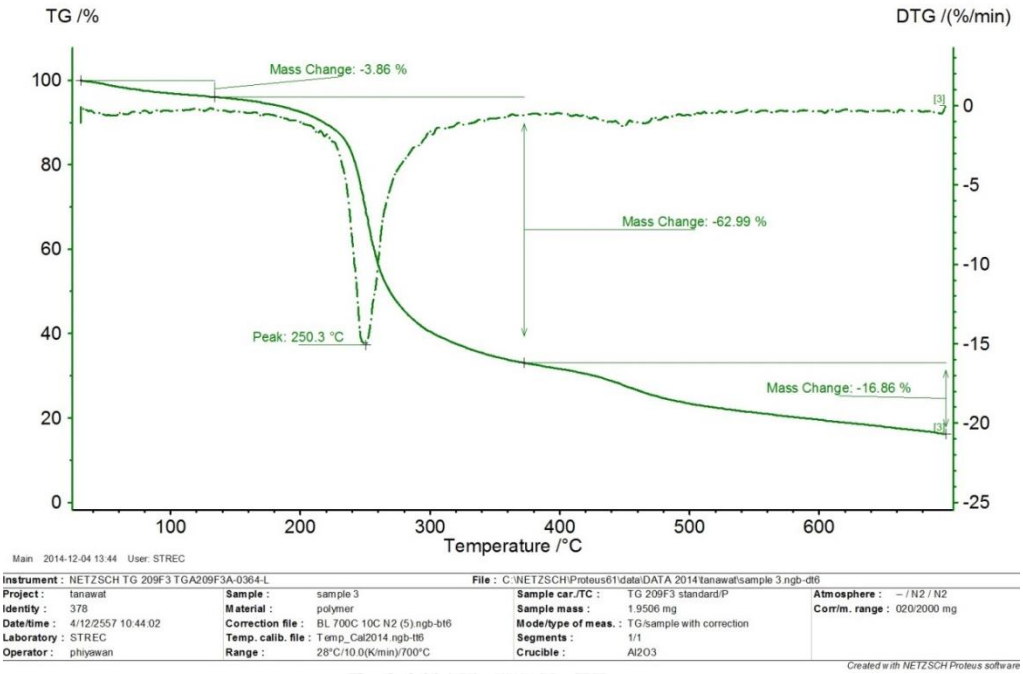

Figure E3 Thermo gravimetric analysis (TGA) curves of minoxidil-grafted cellulose nanoparticles

APPENDIX F

1. 1. Calculation of encapsulation efficiency (% EE) and loading capacity (% loading) of minoxidil encapsulation

The calibration curve of minoxidil was prepared using minoxidil solution in deionized water at concentration 0, 1, 2, 3, 5, 7, 10 and 15 ppm. A calibration curve was plotted between each minoxidil concentration and its corresponding absorbance value as shown in Table F1 and Figure F1. The concentration of minoxidil in sample was determined by comparison to this calibration curve.

Table F1 minoxidil concentration and its corresponding absorbance value at 289 nm

Concentration (ppm)	**0**	**1**	**2**	**3**	**5**	**7**	**10**	**15**
Absorbance at 320 nm	0.000	0.057	0.111	0.165	0.277	0.376	0.547	0.767

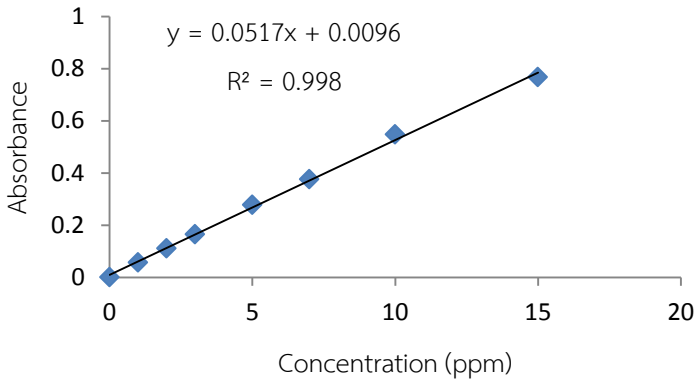

Figure F1 Calibration curve for release study of minoxidil in in deionized water at 289 nm

By plotting a graph between absorbance and concentrations of standard minoxidil solutions, a linear relationship was obtained and used for calculation of concentration of minoxidil.

From the equation of calibration curve;

$$Y = 0.0517X + 0.0096, R^2 = 0.9980 \quad (1)$$

The amount of minoxidil loaded into the nanoparticles was calculated by equation (1);

$$0.091 = 0.0517X + 0.0096$$

$$X = 1.57 \text{ ppm} = 1.57 \text{ mg/L}$$

The amoxicillin diluted one thousand-fold, so the amount of amoxicillin was

$$1.57 \times 1{,}000 = 1{,}570 \text{ mg/L}$$

In final volume of 5 mL had unentrapped minoxidil of (1,570 x 5)/1000 = 7.87 mg

Weight of employed minoxidil and dialdehyde soluble cellulose were 70 and 10 mg

Encapsulation efficiency (%) = (A/B) × 100

Loading (%) = [A/(A+C)] × 100

Whereas A is weight of encapsulated minoxidil = weight of minoxidil used - weight of minoxidil found in filtrated;

B is weight of minoxidil used;

C is weight of polymer used.

- Entrapment efficiency (%EE)

Minoxidil initial used = 70 mg

Minoxidil found in filtrated = 7.87 mg

= ((70-7.87)/70) × 100

= 88.76 %

- % Loading

Weight of encapsulated minoxidil + polymer = 62.13 + 10 mg

Minoxidil found in filtrated = 7.87 mg

= [(70-7.87)/(62.13+10)] × 100

= 86.14 %

APPENDIX G

1. Calculation of % release and of minoxidil in ABS pH 5.5

The calibration curve of minoxidil was prepared using minoxidil solution in ABS pH 5.5 at concentration 0, 1, 3, 5, 7, 10 and 15 ppm. A calibration curve was plotted between each minoxidil concentration and its corresponding absorbance value as shown in Table G1 and Figure G1. The concentration of minoxidil in sample was determined by comparison to this calibration curve.

Table G1 minoxidil concentration and its corresponding absorbance value at 287 nm

Concentration (ppm)	**0**	**1**	**3**	**5**	**7**	**10**	**15**
Absorbance at 320 nm	0.000	0.062	0.185	0.313	0.422	0.619	0.926

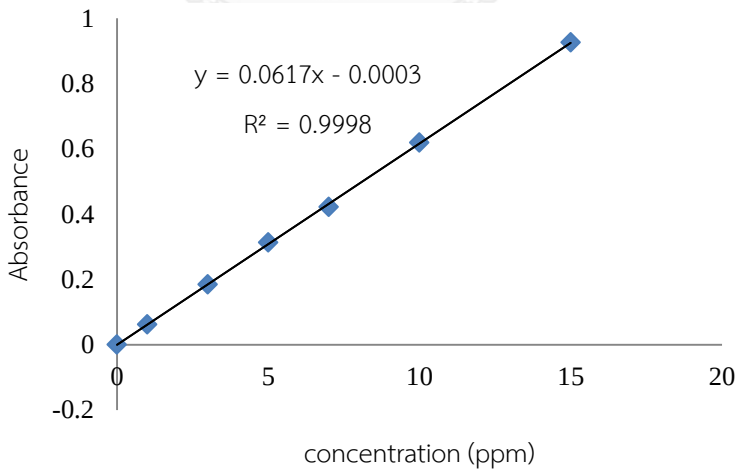

Figure G1 Calibration curve for release study of minoxidil in ABS pH 5.5 at 287 nm

By plotting a graph between absorbance and concentrations of standard minoxidil solutions, a linear relationship was obtained and used for calculation of concentration of minoxidil.

From the equation of calibration curve;

$$Y = 0.0617X - 0.0003, R^2 = 0.9998 \quad (1)$$

1.1 Calculation of % minoxidil release of encapsulated minoxidil in ABS pH 5.5

- Minoxidil in the ABS at 0 h

From equation (1) $Y = 0.0617X - 0.0003$

$0.000 = 0.0617X - 0 .0003$

$X = 0.0049$

Dilution factor = 10 $X = 0.0049 \times 10$

$X = 0.049$ ppm

% minoxidil released at 0 hour: minoxidil initial used = 70 mg

minoxidil found in ABS = 0.049 mg

% minoxidil released = (0.049/70) x 100

= 0.07 %

- Minoxidil in the ABS at 0.5 h

From equation (1) $Y = 0.0617X - 0.0003$

$0.191 = 0.0617X - 0 .0003$

$X = 3.100$

Dilution factor = 10 $X = 3.100 \times 10$

$X = 31.00$ ppm

% minoxidil released at 0.5 hour: minoxidil initial used = 70 mg

minoxidil found in ABS = 31.00 mg

% minoxidil released = (31.00 /70) x 100

= 44.29 %

- Minoxidil in the ABS at 1 h

From equation (1) Y = 0.0617X - 0.0003

0.282 = 0.0617X - 0 .0003

X = 4.575

Dilution factor = 10 X = 4.575 x 10

X = 45.75 ppm

% minoxidil released at 1 hour: minoxidil initial used = 70 mg

minoxidil found in ABS = 45.75 mg

% minoxidil released = (45.75 /70) x 100

= 65.36 %

- Minoxidil in the ABS at 2 h

From equation (1) Y = 0.0617X - 0.0003

0.353 = 0.0617X - 0 .0003

X = 5.726

Dilution factor = 10 X = 5.726 x 10

X = 57.26 ppm

% minoxidil released at 2 hour: minoxidil initial used = 70 mg

minoxidil found in ABS = 57.26 mg

% minoxidil released = (57.26 /70) x 100

= 81.80 %

- Minoxidil in the ABS at 3 h

From equation (1) $Y = 0.0617X - 0.0003$

$0.372 = 0.0617X - 0 .0003$

$X = 6.034$

Dilution factor = 10 $X = 6.034 \times 10$

$X = 60.34$ ppm

% minoxidil released at 3 hour: minoxidil initial used = 70 mg

minoxidil found in ABS = 60.34 mg

% minoxidil released = (60.34 /70) x 100

= 86.20 %

- Minoxidil in the ABS at 4 h

From equation (1) $Y = 0.0617X - 0.0003$

$0.387 = 0.0617X - 0 .0003$

$X = 6.277$

Dilution factor = 10 $X = 6.277 \times 10$

$X = 62.77$ ppm

% minoxidil released at 4 hour: minoxidil initial used = 70 mg

minoxidil found in ABS = 62.77 mg

% minoxidil released = (62.77 /70) x 100

= 89.67%

- Minoxidil in the ABS at 5 h

From equation (1) Y = 0.0617X - 0.0003

0.392 = 0.0617X - 0 .0003

X = 6.358

Dilution factor = 10 X = 6.358 x 10

X = 63.58ppm

% minoxidil released at 5 hour: minoxidil initial used = 70 mg

minoxidil found in ABS = 63.58 mg

% minoxidil released = (63.58/70) x 100

= 90.83 %

- Minoxidil in the ABS at 6 h

From equation (1) Y = 0.0617X - 0.0003

0.401 = 0.0617X - 0 .0003

X = 6.504

Dilution factor = 10 X = 6.504 x 10

X = 65.04ppm

% minoxidil released at 6 hour: minoxidil initial used = 70 mg

minoxidil found in ABS = 65.04 mg

% minoxidil released = (65.04/70) x 100

= 92.92 %

- Minoxidil in the ABS at 24 h

From equation (1) Y = 0.0617X - 0.0003

0.428 = 0.0617X - 0 .0003

X = 6.942

Dilution factor = 10 X = 6.942 x 10

X = 69.42ppm

% minoxidil released at 24 hour: minoxidil initial used = 70 mg

minoxidil found in ABS = 69.42 mg

% minoxidil released = (69.42/70) x 100

= 99.16 %

VITA

Mr. Adison Treemak was born on May 10, 1988 in Bangkok, Thailand. He received a Bachelor's Degree of Science in Industrial Chemistry Analytical Instrumentation from King Mongkut's Institute of Technology Ladkrabang in 2010. And then, he started his graduate study a Master's Degree in the Program of Petrochemistry and Polymer Science, Faculty of Science, Chulalongkorn University. During master degree study, he had an opportunity to present his work in poster session in the topic of "Modification of Pineapple Fiber and Application in Drug Delivery" at Macro 2014. Chiang Mai, Thailand of which he got an award as Best Poster Award (2nd Prize) in Polymeric-based Carriers for Medical and Cosmetic Applications field. The finance for joining the conference was supported by the Graduate school, Chulalongkorn University.

His present address is 502/174, Decha-Tungka road, Donmuang, Bangkok Thailand 10210.